Wavelike 3-Spherical Lorentz Transformations in M^5 : Cosmological Applications of Huygens-Fresnel Wave Theory

M.G. Ifans

"Our universe has many special and (to us at least) surprising properties that we want to evaluate in order to see if they could have been otherwise. This means that we have to be able to produce examples of 'other' universes so as to carry out comparisons." John D. Barrow, *The Book of Universes*

Abstract

The modern theoretical picture of critical cosmological density with spatially flat physical geometry can be described in terms of spherical wave physics over a range of scales. The Lorentz transform is wavelike; for example de Broglie particles behave as wave groups with phase speed deriving from the Minkowski geometry. Relativistic waveforms are also found in astrophysical and cosmological theories. Here a 5D *expansion process is developed on an equidistant* * *manifold in steady-state wavelike expansion, formulated with Huygens' principle as a locally concentric, polar Lorentz transformation. Derived particle wavelets are similar to the Schwarzschild metric at stellar scales, and to the Friedmann equations at cosmological scales. Metrics and null trajectories are derived as functions of the open spherical plane wavefront, extending outwards on an affine connection deriving from the flat and wavelike Lorentz transform. The conformal energetic* 4*-space metric has a dilated time-scale with* ΛCDM*-like physical geometry. This* 5D *process is tested on standard-model expansion and energy density data. The resulting tractable and consistent inflationary process is summarised with derivations and empirical tests.*

Quantum wavefunction models of general-relativistic cosmologies have established that wave-packet evolution can simulate cosmological expansion [1], with recognisable features such as evolving cosmic acceleration at epochal inflections. This research series will examine and parameterise a flat cosmology of the wave-theoretic type, with a re-examination of the consistency of cosmological acceleration in a plane waveform theory. Equidistant projections in the lead c-constant candidate reduce cosmological accelerations to zero, with flat geometric dilutions of magnitude plus Lorentz dilations of recession that develop apparent energies equivalent to acceleration. The resulting dark-emergent cosmology is an independent concept unlike any described in a recent historical review of scientific cosmologies [2].

Construction of Huygens-Lorentz Transformations

The Lorentz transformation can be systematically reconstructed to provide a consistent flat spacetime metric with a wavelike expansion front. This section presents the key step, a symmetric dilation of space and time axes inherent in the Minkowski geometry, which inverts the spacetime into a Euclidean 3-spherical relative spacetime with a polar expanding lightcone. The SR magnitude of any expansion-radiation 4-velocity remains exactly $|U| = c$.

Particle Model

The key feature is the right-triangular construction of a spacetime interval. This controls integral elements of the spacetime such that the local, astrophysical and cosmological extensions of the theory are continuously wavelike and flat, with similar structure at every scale. This spacetime can be derived from the relativistic principles of the de Broglie wave-particle or momentum-wavelength theory [11]. I will re-derive in some detail the de Broglie phase relationships and examine the fit to this geometric and physical transformation of the Minkowski diagram onto a Euclidean plane.

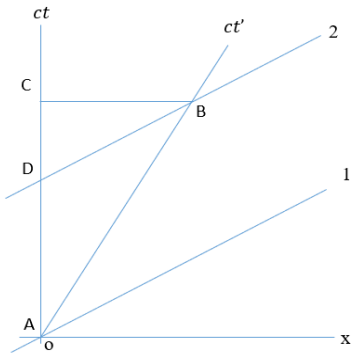

$$E = \gamma mc^2 = hf \qquad 5$$

hence a particle at rest has a proper interval:

$$T_0 = 1/f_0 = h/mc^2 \qquad 6$$

In this Minkowski diagram, $\overline{AB} = cT_0$ is the proper interval between axes 1 and 2 of equal and constant phase, such that a particle, as a quantized oscillator, remains continuously in phase with a wave that follows the Lorentz transform:

$$(\overline{AB})^2 = (\overline{AC})^2 - (\overline{CB})^2 = (cT_0)^2 \qquad 7$$

Figure 3 (from de Broglie [11]) *"This result is a simple application of trigonometry; whenever, we emphasize, trigonometry is used on the plane* xot*, it is vitally necessary to keep in mind that there is a particular anisotropism of this plane."*

The Minkowski space axis is a locus of constant phase for a wave in motion on a spacelike trajectory, while the particle is an in-phase "periodic phenomenon", i.e. an oscillator or wave group in motion on a timelike trajectory:

"One may imagine that, by cause of a meta law of Nature, to each portion of energy with a proper mass m_o, one may associate a periodic phenomenon of frequency f_0, such that

$$hf_0 = m_0c^2$$

measured in the rest frame of the energy packet."

* An equidistant projection, equivalent to a flat arc-length metric on a polar co-moving coordinate ψ, with redshift $z = e^{\psi} - 1$.

de Broglie points out that there are, or were at the time, two different ways of calculating the frequency of a particle in motion:

1) The period dilates to a longer time (lower frequency) due to the Lorentz transformation:

$$f = \frac{f_0}{\gamma} = \frac{m_0 c^2}{\gamma h} = \frac{m_0 c^2 \sqrt{1-\beta^2}}{h} \qquad \textit{particle time dilation}$$

and/or

2) The energy dilates to a higher frequency due to Planck's law:

$$E = hf = \gamma m_0 c^2$$

$$f = \frac{\gamma m_0 c^2}{h} = \frac{m_0 c^2}{h\sqrt{1-\beta^2}} \qquad \textit{particle energy dilation}$$

Suppose at $(x,t) = (0\,,0)$ the periodic phenomenon and wave have equal phase. Later at time t the particle has moved a distance x and loses phase compared to a stationary origin RF since it is time-dilated by γ so its proper frequency is reduced.

$$x = vt = \beta ct \qquad \text{at frequency} \qquad f = \frac{m_0 c^2}{\gamma h} \qquad \textit{on the trajectory}$$

8

So the time-dilated oscillator's phase at x has evolved to

$$ft = \frac{t}{T} = \frac{m_0 c^2}{\gamma h} t = \frac{m_0 c^2}{\gamma h} \frac{x}{\beta c} \qquad 9$$

$$= 0,1,2 \ldots \qquad \textit{phase number on } 2\pi \textit{ (oscillator)}$$

Likewise the phase of the wave at coordinate (x,t) evolves $\Delta t = t(x) - \beta x/c$ between successive common phases along the Minkowski axis $t = \frac{vx}{c^2} = \frac{\beta}{c} x$ with energy dilation due to Planck's law:

$$f'\,\Delta t = \frac{\gamma m_0 c^2}{h}\left(\frac{x}{\beta c} - x\frac{\beta}{c}\right) \qquad \textit{between trajectory and M space axis}$$

$$= \frac{\gamma m_0 c^2}{h} \frac{x}{\beta c}(1-\beta^2) = \frac{m_0 c^2}{\gamma h} \frac{x}{\beta c} \qquad \text{same phase } \textit{as time dilated oscillator at any } (x,t) \qquad 10$$

The phase-group relationship can be obtained in general terms:

$$U = \frac{df}{d\left(\frac{f}{V}\right)} \qquad 11$$

Where U is the group speed and $V = V(f)$ is the phase speed as a function of the frequency. Assuming a particle is a wave group whose phase follows the Minkowski axis, the phase speed $V = x/t = x/(vx/c^2) = c/\beta$:

$$f = \frac{\gamma m_0 c^2}{h} = \frac{m_0 c^2}{h\sqrt{1-\beta^2}} \qquad V = \frac{c}{\beta} \qquad \frac{f}{V} = \frac{m_0 c^2 \beta}{hc\sqrt{1-\beta^2}} \qquad 12$$

We can write this in terms of partials, or simpler:

$$U = \frac{df}{d\left(\frac{f}{V}\right)} = \frac{\frac{df}{d\beta}}{\frac{d\left(\frac{f}{V}\right)}{d\beta}} \qquad 13$$

so $\frac{df}{d\beta} = \frac{m_0 c^2}{h} \frac{\beta}{(1-\beta^2)^{3/2}}$ ①

and $\frac{d\left(\frac{f}{V}\right)}{d\beta} = \frac{m_0 c^2}{hc} \frac{1}{(1-\beta^2)^{3/2}}$ ②

or $U = \frac{①}{②} = c\beta = v \qquad 14$

where v is the particle velocity, now unquestionably a group speed $c\beta$ to a phase speed c/β.

hence $\lambda = \frac{V}{f} = VT = \frac{c}{\beta}\frac{h}{\gamma m_0 c^2} = \frac{h}{\gamma m_0 v}$ *de Broglie particle wavelength* 15

We can also think of the particle as having a wavelength of period T in time, which would be the period plotted vertically on the Minkowski diagram:

$$cT = \frac{h}{\gamma m_0 c} \qquad \text{nb } \lambda f = \frac{\lambda}{T} = v_{phase} = \frac{h}{\gamma m v}\frac{\gamma m c^2}{h} = \frac{c^2}{v} = \frac{c}{\beta} \qquad 15.5$$

The denominator terms $(\gamma mc, \gamma mv)$ are recognisable in the modern formulation of special relativity as the 4-momentum:

$$\lambda^\mu = hk^\mu \qquad \text{where the } k \text{ are inversions of momentum in all spacetime directions.} \qquad 16$$

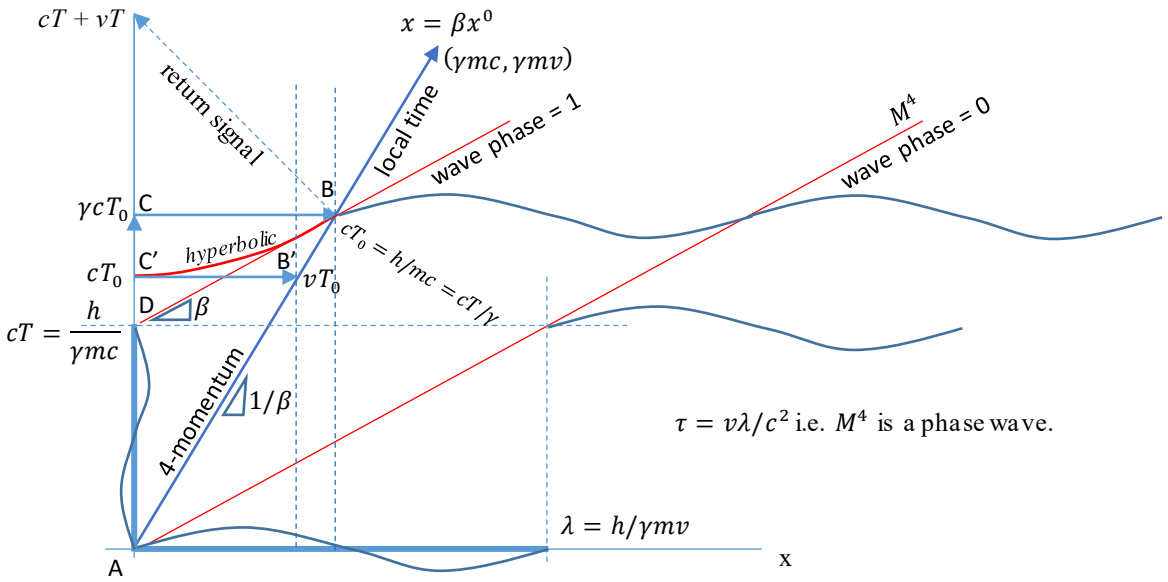

Figure 5: *In-phase spacetime wavelengths to scale, with a natural construction on adjacent phase-linked space axes.*

The frequency of the energy-dilated particle at D must carry the energy through that space:

$$E = hf' \qquad 17$$

where $$f' = \frac{1}{T'} = \frac{\gamma}{T_0} = \frac{\gamma m c^2}{h} \qquad 18$$

The wavelengths in Figure 5 are thus correctly to scale in the stationary observer's reference frame. The hyperbolic proper time cannot be drawn to scale, i.e. the proportions of cT_0 and $h/\gamma mc$ as shown are not exact in this Euclidean plane.

The proper interval cT_0 can be drawn to scale in wavelength and period by a flat transformation of the Euclidean plane. This can be done in a single geometric step with a physical interpretation that follows from wave theory:

As in Figure 6, project a spherical wavelet (–) from a moving particle to the stationary ct axis. The dilated frequency cT_0/γ now projects onto the ct axis as a cosine at D. *The corresponding wakelet (–) relates the time-dilated particle E to the stationary RF at* C′ *along the travel distance (←) rotated through the same angle. The construction is to scale and symmetric.*

The rotated proper interval $\overline{\mathrm{AE}} = h/\gamma mc$ is now square to $\overline{\mathrm{C'E}} = \overline{\mathrm{C'B'}}$ and is involved in a flat Pythagorean sum of the stationary space and time coordinates, identical to the spacetime interval calculation, but plotted to scale in the plane:

$$(\overline{\mathrm{AE}})^2 = \left(\overline{\mathrm{AC'}}\right)^2 - \left(\overline{\mathrm{CB'}}\right)^2 = (cT_0)^2 - (vT_0)^2 = (cT_0/\gamma)^2 \qquad \textit{spacetime in plane circular trigonometry} \qquad 19$$

The right angle at E is a transformation of the spacetime intersection at B′ by rotating the proper co-moving distance $\overline{\mathrm{C'B'}}$, onto the polar distance $\overline{\mathrm{C'E}}$, which preserves relative velocity between the stationary and moving frames. The new trajectory has a natural formula $x = \gamma\beta x^0$ that follows from the dilation. The particle echoes at E and B′ are synchronised and dilated.

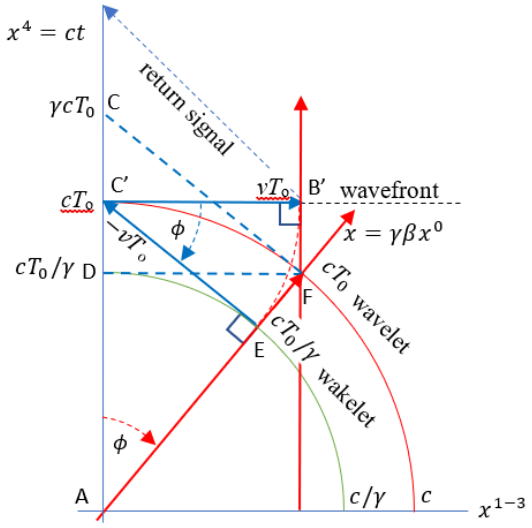

the rotation angle ϕ has simple trigonometric projections:

$$vT_0 = cT_0 \sin\phi \qquad 20$$

$$\sin\phi = v/c = \beta \qquad 21$$

$$\cos\phi = \sqrt{1 - \sin^2\phi} = 1/\gamma \qquad 22$$

and $$\tan\phi = \gamma\beta \qquad 23$$

$$(\overline{\mathrm{AE}})^2 = \left(\overline{\mathrm{AC'}}\right)^2 - \left(\overline{\mathrm{CB'}}\right)^2 \qquad 24$$

In this construction, a dilated particle E in the wakelet interferes onto the wavefront at B′. E lags behind cT_0 but has the same phase in space.

Figure 6: *Take the spacetime intersection at* B′ *and rotate it to* E, *reversing the relative velocity. This shows all the stationary and moving lengths and intervals to exact scale drawn on a flat page.*

The de Broglie theory is a realisation that special relativity and its geometry are wavelike. It is useful to identify other wavelike characteristics, for instance to consider how point E might physically transform to B′. A version of Huygens-Fresnel

interference onto the secondary wavefront is an obvious interpretation, so long as the dimension of the ct axis is a *space* in the complete sense, not just an expression of velocity-time. The controlling t-parameter is then *external* [63].

The dilation of the proper interval by its gradual lag behind the observer can be interpreted as a nonlinear "wake" typical of gravitational waves† [62] and of Huygens wavelets in 4D [45]. The wavelet, wakelet and secondary wavefront in Figure 6 are all concurrent and affine-connected in Figure 8 as they interfere onto the secondary wavefront: E and B' are in phase, as are F and C'. The phase wave's energy is dilated equally as the particle's time is dilated.

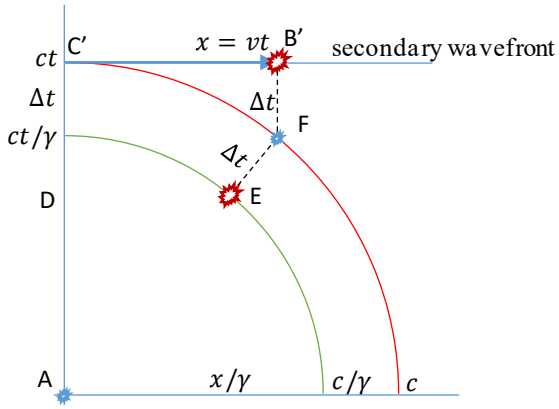

The dilated particle observed at B' is in phase with E, which evolves as a 4D wake triggered by the intersection at A and lagging an increasing Δt behind F. The lag is such that E has the same phase that F had at that point. The dual-wave manifold structure can be pictured as a particle and wake at a given instant: the particle F is in phase with C' and coexists with the dilated wake E and secondary wavefront C'B'. The external time parameter of the evolving geometry is separate from but correlated to the expanding spatial axis. This is a four-dimensional space at one instant of 5th D time.

Figure 8: *Huygens wavelets in* 4D *have a non-linear wake, applied here to model time dilation effects.* (desmos)

The moving particle and stationary observer evolve on coherent wavelets expanding at c from the intersection at A, so the particle has travelled the contracted distance $x/\gamma = vt_o = vt/\gamma$ in its own proper time t_o and also the full $x = vt$ in the observer's local time $t = \gamma t_o$, with no anisotropy. This would apply to macroscopic bodies in motion as per special relativity.

Spherical Gravitation Model

The model is also consistent with the Schwarzschild metric [12], as a first approximation on scales from planetary to intergalactic, by systems of gravitating-expanding point masses with polar waveforms. Voids and filamentary intergalactic matter in sub-cosmological gravitation fields are reasonably idealised by isolated centres of mass at the intermediate scale, while at larger scales the spacetime is isotropic-homogeneous and effectively flat.

The consistency of the general and special waveform models is demonstrated by writing the null Schwarzschild metric in a polar form with gravitational redshift factors. The result has the same rotated transform structure, that can be plotted as gravitational-redshifted 3-spherical wavelets with the same degrees of symmetry plus non-linearities:

$$ds^2 = \cancel{d\chi^2}^{\,0} - c^2d\tau^2 = r^2\cancel{d\Omega^2}^{\,0} + \frac{dr^2}{\left(1-\frac{2GM}{c^2r}\right)} - c^2dt^2\left(1-\frac{2GM}{c^2r}\right) \qquad \textit{Schwarzschild local null metric} \qquad 28$$

i.e.

$$(cd\tau)^2 + (\gamma_G dr)^2 = (cdt/\gamma_G)^2 \qquad \textit{Schwarzschild polar null metric} \qquad 29$$

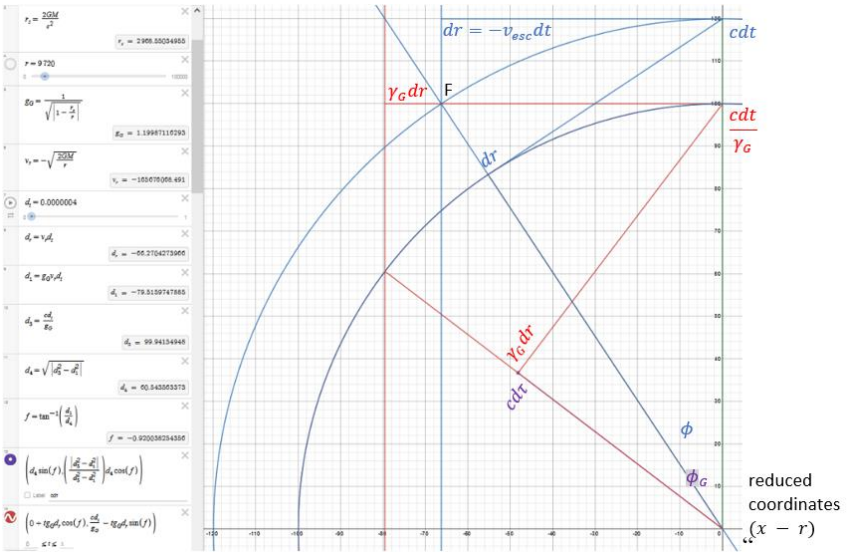

Figure 11: *A test mass free-falling onto a stellar-mass black hole at e.g.* $r = 3.3R_s$ *against an inertial frame in flat space at a constant velocity, arbitrarily illustrated at the free-fall velocity. The* $dr \ldots cdt$ *show* SR *effects at that velocity in flat spacetime as per Figures* 2 *and* 3*, while the redshifted* $\gamma_G\, dr$ *show the nonlinear effects of the spherical gravitational field at*

† Electromagnetic waves in gravitational fields also develop a wake [62].

that radius. The intersection at F *of free and redshifted models occurs when the escape velocity is explained by a connection to the* SR *flat space at that speed* (GR). *Also as* $r \to \infty$ *the nonlinear geometry reduces to flat* SR i.e. $\gamma_G\, dr \to dr$ *as* $v_{esc} \to 0$.

https://www.desmos.com/calculator/db2ihe5nlp

The affine or timelike connection inferred by the delay-dilation, which coordinates a constructive interference, can be derived by GR methods [III] and Appendix 2: the null-metric Christoffel connection obtains a single parameter, the external time in direct and inverse proportions. The 4-space in x^0 action is suggestive of Kaluz-Klein theory with a graviton in the 4D.

Cosmological Extension of Relativistic Wave Model via Huygens' Principle

The underlying wavelike structure follows from de Broglie (SR) and Schwarzschild (GR) theories, and is energetically and geometrically flat in accord with cosmological observations. The infinitesimals of this model would integrate directly to cosmological totals, without the need to construct general connections since the spacetime is claimed to be flat at all relevant scales. This provides a means of directly measuring energy densities at any distance in a flat universe of this type.

An important condition on the Huygens-Fresnel analogy is that Huygens' wavelets travel in 3D space in all forward directions, while in this model the expansion direction is a space matched dimensionally to time. If that is a real physical space, then this expansion has 4 space dimensions evolving in time, 5 dimensions in all. The theoretical graviton is 4-dimensional [64]. In 4 space dimensions the wavefront must be a gravitational field. It is consistent that Huygens' principle is non-linear in 4D, or in any even-numbered space dimensionality [44].

Also like gravity, a meta law based on Huygens' Principle is capable of developing a curved, hyperspherical Riemannian manifold, suggesting the equivalence of a spherical wavefront to an expanding flat gravitational curvature:

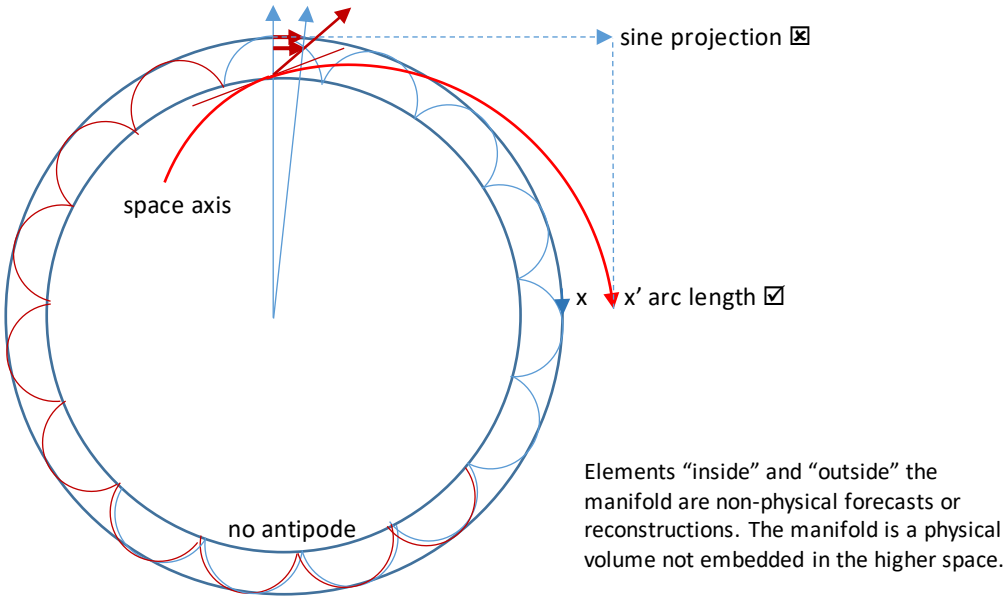

Figure 12: *A hyperspherical wavelike universe identical to a flat universe with gravitational curvature. This can be spherical* and *flat i.e.* open *so long as any reference frame's antipodal distances do not join up smoothly*.

Using Guth's notation [13], we can compare a physical or past distance l_p to a coordinate distance l_c on the manifold by a time-variable cosmological scale factor a, the ratio of co-moving distances and/or Hubble radii at past and present times. The equivalence of new terms introduced to follow this correspondence are highlighted ≡ by these definitions:

$$l_p = a(t)\, l_c \equiv r = S\psi \quad \text{where} \quad a(t) = \frac{l_p}{l_c} \equiv \frac{r}{r_o} = \frac{S}{S_o} \quad \text{and} \quad l_c \equiv S_o\psi = r_o \qquad 30$$

Co-moving coordinates are here measured not in notches [13] or boxes (Susskind [14]) but in open radians.

A wavelike Huygens-Lorentz construct provides two differential equations for the behaviour of light and gravity radiation in expansion: A 4D component $dS = cdt$ that expands at light speed, and a 3D component of radiation and particle motion in the manifold's spherical 3-space at $dr = Sd\psi = cdt$.

- Hubble radius manifold $S = ct$ expands 4-spatially in time at constant velocity c;
- Radiation and gravitation propagate 3-spatially as $x = c\Delta t$ at constant velocity c.

Stated as hypotheses $S = ct$ and $x = c\Delta t$ we find two c-valued differential equations defining the lightcone:

$$\frac{dS}{dt} = c \qquad \textit{Constant concentric expansion of hypothetical 4D Hubble radius } S = ct \qquad \mathbf{31}$$

and $dx = cdt = Sd\psi$ *Local* 3D *light cone distance elements in polar coordinates*

or $$\frac{d\psi}{dt} = \frac{c}{S} \qquad \textit{Decreasing coordinate velocity of radiation in 3-Space} \qquad \mathbf{32}$$

$$\frac{dS}{d\psi} = \frac{dS}{dt}\frac{dt}{d\psi} = c\frac{S}{c} = S \qquad 33$$

Eqn 33 is a standard problem in polar coordinates; the solution is a logarithmic (growth) spiral:

$$\frac{dS}{S} = d\psi$$

or $\ln\left(\frac{S_o}{S}\right) = \psi$ where S is an initial condition on the present observer's S_o 34

$$\frac{S_o}{S} = e^{\psi}$$ 35

or $\frac{S}{S_o} = a = e^{-\psi}$ *past/present Hubble radii, scale factor and co-moving coordinate* 36

An observer at O (Figure 14) looking telescopically in any direction would see photons from continually distant astronomical and cosmological events in that direction, arriving at that moment. The locus of immediately visible events along that line of sight, i.e. a light cone null axis, would overlap with the physical path of the most distant radiation, arriving coherently with all other distant sources in that observation. This locus derives by integrating Eqns 31 and 32 as radial and angular motions:

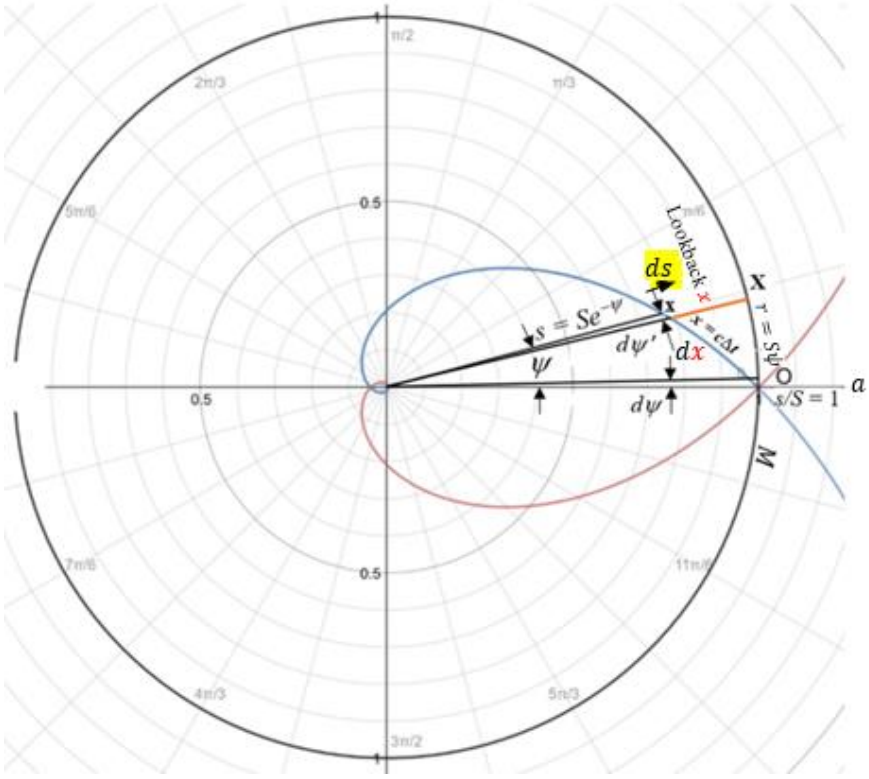

Figure 14: *A light cone develops as a* 1:1 *logarithmic graph, a* 4D *reconstruction of past spacetime. All events on the forward view from* O *along* x *to galaxy* **X** *are visible to* O *at that instant. The light cone is* 1:1 *conical in the limit of small distances near the observer, where radiation and gravitation cross the observer's world-line. A galaxy at co-moving coordinate* ψ *is located at* X *in physical observable space* M *and at* **X** *as an image on the light cone, at a visible distance* $x = c\Delta t$*. The spiral light-cone is non-physical, a geometric construction; the open spherical manifold is real in the co-moving sense, and not unique.*

Integration of curvatures on this expansion-relativistic curvature derive a lookback time and distance that is equivalent to the proper interval along the lightcone, as follows:

Conventional Lookback Distances and Times in Visible Spacetime

A 3D distance (orthogonal to S) is found by integration of contravariant arc lengths in the manifold $M \perp S$:

$$dx = dr = cdt = Sd\psi = S_0 e^{-\psi} d\psi$$ *element of 3-distance arc length* dx *orthogonal to 4-radius* S 37

Integrated proper distances corresponding to the light cone (signal distance) are then a straightforward result:

$$x = \int_0^{\psi} S d\psi = \int_0^{\psi} S_0 e^{-\psi} d\psi$$ 38

$$= S_0\left(1 - e^{-\psi}\right)$$ *integrated distance along a lightcone* 39

$$= S_0 - S$$ *radial increment of distance* 40

$$= ct_0 - ct$$

i.e. $x = c\Delta t = c\tau$ *conventional look-back distance and interval* 41

$\rightarrow S_0 = ct_0$ as $\psi \rightarrow \infty$ *a maximum 3D distance: the present Hubble radius* 42

The distance x in visible space thus corresponds to the proper distance along a photon's path. A galaxy observed in epoch t at distance $x = c\Delta t$ is seen at $t_0 - t = \Delta t$ years ago. This accords with the conventional physics of radiation, but derives as a three-dimensional arc length, a complement to Hubble radius, *and* a light travel time.

Recession

The time-derivative of distance at a co-moving coordinate is a recession velocity equivalent to Hubble expansion. This is developed by a chain-rule differentiation of distance with time:

$$\frac{dx}{dt} = \frac{\partial x}{\partial S_0}\frac{dS_0}{dt} + \frac{\partial x}{\partial \psi}\frac{d\psi}{dt}^{0} \qquad \psi \text{ is constant for co-moving coordinates} \qquad 43$$

Given $S = ct$ and $x = S_0(1 - e^{-\psi})$ (Eqns 31, 39)

$$\frac{dx}{dt} = \frac{\partial x}{\partial S_0}\frac{dS_0}{dt} = c(1 - e^{-\psi}) = c\frac{x}{S_0} = \frac{c}{ct_0}x = \frac{x}{t_0} = H_0 x \qquad 44$$

This rate of distance increase is the measurable (visible) recession velocity, which is proportional to distance as per a t^{-1} Hubble law that incorporates the scale factor a and conventional redshift z:

$$v_x = c(1 - e^{-\psi}) = c(1 - a) = ca(a^{-1} - 1) = caz = H_0 x \qquad \textit{visible recession velocity} \qquad 45$$

As first proposed by de Sitter [19] in response to Slipher [20, 21], then theoretically re-located by Friedmann [22] and Lemaître [23] and finally confirmed observationally by Hubble in 1929 [24], visible timescales at great distances are altered by redshift due to recession proportional to distance:

Since $x = S_0(1 - e^{-\psi})$ (Eqn 39)

then $\frac{dx}{dt} = v_x = c(1 - e^{-\psi}) = \frac{c}{S_0}x$ *Hubble recession velocity* (Eqn 44)

i.e. $H_0 = \frac{c}{S_0} = \frac{d\psi}{dt} = \frac{c}{ct_0} = \frac{1}{t_0}$ *Hubble universal time and angular velocity* 46

This predicts a slightly greater age of the universe. Using the measured value‡ of H_0, $H_0 = 67.7$ km.s^{-1}MPc^{-1} or $H_0 = 2.194 \times 10^{-18}$ s^{-1} at 3.086×10^{19} km.MPc^{-1} we obtain:

$$t_0 = \frac{1}{H_0} = \frac{1}{2.194 \times 10^{-18}}$$

$= 4.558 \times 10^{17}$ s = 14.44×10^9 years§ *re-estimated universal age* 63

or $S_0 = 1.366 \times 10^{26}$ m *re-estimated Hubble Radius* 64

Redshift Effects of Recession Velocity: Doppler Scale Factor

The exponential variable $e^{-\psi}$ is the cosmological scale factor a at any co-moving coordinate, which in the standard model is the dominant redshift effect at large coordinates. The effect has been identified (Eqn 52) as an a-scaled and hence dilated visible evolution of an observed coordinate:

$$\frac{dS}{dt} = ac \text{ visible recession compared to present epoch}, S = S_o e^{-\psi} \text{ and } \frac{dS_o}{dt} = c \qquad \text{(Eqn 52)}$$

The cosmological redshift is found by differentiating past reference frames S to the present era S_o:

For $S = S_0 e^{-\psi}$ at constant ψ, (Eqn 36)

$$\frac{dS}{dS_0} = e^{-\psi} = a \qquad \textit{frequency redshift by derivative of past to present RF} \qquad 65$$

as $$\frac{dS}{dS_0} = \frac{\frac{dS}{dt}}{\frac{dS_0}{dt}} \qquad \textit{scaled evolution of two frames as relative frequencies} \qquad 66$$

Both S and S_0 are functions of time, hence the redshift is the ratio of proper time scale and evolution rate in visible past to present. This proper time is modified in [III] by relative dilations conforming to ΛCDM.

The recession analysis (Eqn 45) shows that the scale factor is also a low-velocity relativistic Doppler effect due to recession velocity:

$$v_x = c(1 - e^{-\psi}) \qquad \text{(Eqn 45)}$$

so $$a = e^{-\psi} = 1 - v_x/c = 1 - \beta_x \qquad 67$$

This has the form of a Doppler effect, lacking a Lorentz-FitzGerald gamma. A co-moving recession velocity derives the same from an expansion of the special relativity of proper or peculiar motion over very large distances. Expansion follows a Huygens wave model with a natural gamma contraction onto a wake.

Section III examines the general metric of this energetic curvature with dilation effects at the cosmological scale.

The following section examines an extension of the wavelike Lorentz transform onto the spherical-wave cosmology by Huygens principle. Reference frames are updated onto the manifold by constructive interference of a delaying wake producing the effect of time dilation. A particle with relativistic peculiar motion, i.e. in intergalactic motion over billions of years, carries that effect as an integral of the dilation process over the spiral curvatures of motion.

---

‡ Later figures from Planck and SDSS-III BOSS have $H_0 = 67.6$ to 67.8 km.s^{-1}MPc^{-1}

§ The more recent estimate $H_0 = 67.8$ km.s^{-1}Mpc^{-1} gives $t_o = 14.42 \times 10^9$ years

Relativistic Peculiar Motion: Effects on Redshift

Eqns 31 and 32 define the motion of radiation and gravitation with expansion; a generalized light cone:

$$\frac{dS}{dt} = c \quad \text{and} \quad S\frac{d\psi}{dt} = c \qquad \text{(Eqns 31, 32)}$$

Similarly the peculiar motion of a particle P at velocity v in expansion at c would describe a trajectory:

$$\frac{dS_P}{dt} = c \quad \text{and} \quad S_P\frac{d\psi_P}{dt} = v \qquad \text{i.e. velocity as per the angular motion of the particle} \qquad 69$$

where ψ_P is the moving coordinate to the trajectory radius S_P of a moving body P. A particle trajectory derives by the same ratio combination of these DEs:

$$\frac{d\psi_P}{dS_P} = \frac{v}{cS_P} \qquad 70$$

So $$\frac{c}{v}d\psi_P = \frac{dS_P}{S_P} \quad \Rightarrow S_P = S_1 e^{\frac{c}{v}\psi_P} = S_1 e^{\frac{1}{\beta}\psi_P} \qquad \textit{trajectory – see} \text{ Figure 16} \qquad 71$$

where S_1 is any initial Hubble radius $S_1 = ct_1$. The particle trajectory is a relative time axis in polar co-moving coordinates. Assuming the Minkowski formulation of SR, there must be a forward space axis scaled inversely to the trajectory. Without assuming any Lorentz coefficients on this axis, the inverse rate constant gives a space axis:

$$S_X = S_1 e^{\beta\psi_P} \qquad \textit{Minkowski space axis – see} \text{ Figure 16} \qquad 72$$

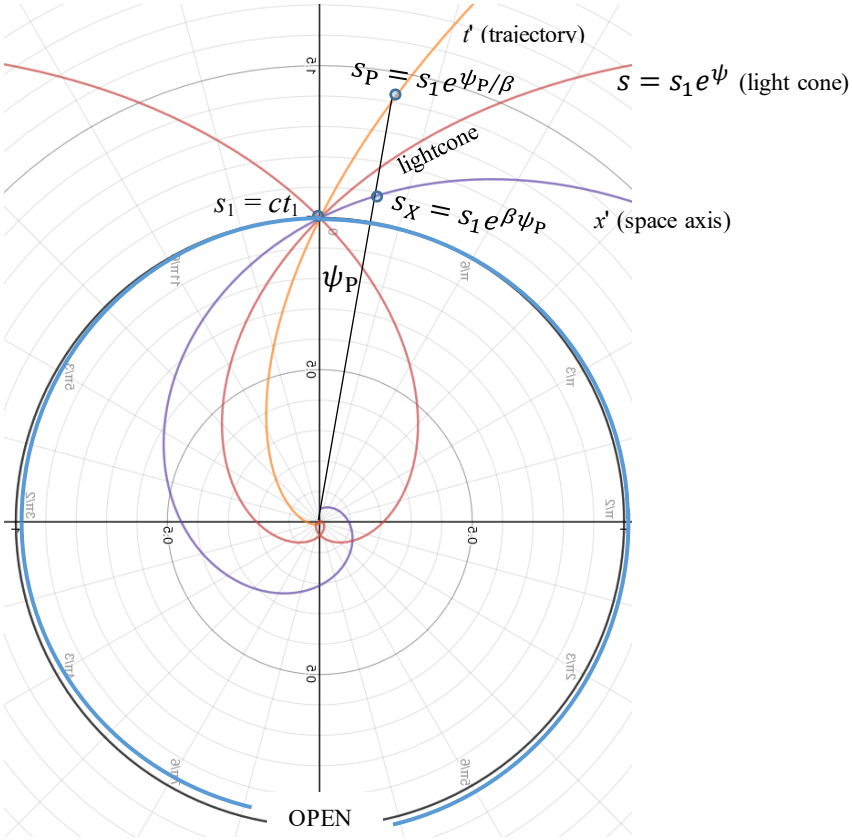

Figure 16: *Cosmological expansion with lightcone, trajectory and Minkowski space axis. The space and time axes conform to special relativity in the construction of Lorentz transforms. At low peculiar velocities the trajectory and space axis tend to radial and circumferential lines. As* $v \to c$ *both graphs align with the light cone. Co-moving observers share a common era defined by the spherical manifold, however a travelling observer at even small speed would define simultaneity on the shallow spiral* (blue) *space axis that diverges from any other observer. This implies that the antipodal point is not closed, i.e. co-moving coordinates in both visible and observable space are infinite beyond* $\psi = \pi$. *In* [III] *we find* $\psi' \to \pi$ *as* $\psi \to \infty$.

Huygens-Lorentz Co-moving Coordinate Transformation

A redshift combining cosmological and peculiar motion is derived from the Huygens-Lorentz construction. Space and time axes are independently dilated to polar axes by γ effects as in Figure 6, extended to a spherical cosmos in Figure 17. This produces contractions of the co-moving coordinate and its functions such as distance and redshift.

The contraction may be obtained from first principles by re-stating Eqn 69 with dilation of elements in the space and time directions respectively. In stellar to nearby intergalactic space, these are the coordinates of Figure 6. At larger scales the polar trajectory develops a dilated co-moving angular velocity and general curvature as in Figure 17:

$$\frac{S_{P'}}{\gamma}\frac{d\psi_{P'}}{dt} = v \quad \text{and} \quad \frac{dS_{P'}}{dt} = c \quad \Rightarrow \quad S_{P'} = S_1 e^{\frac{c}{\gamma v}\psi_{P'}} = S_i e^{\frac{(v)}{\gamma\beta}\psi_{P'}} \qquad 73$$

where $\langle v \rangle$ is the sign $\pm$ of the velocity relative to source $S_i = S_1$ or arrival $S_i = S_2$: $\langle v \rangle = -1$ on approach.

The polar space axis is inverse to the polar trajectory, as is the Minkowski axis to the Galilean trajectory. This is developed by inverting the trajectory terms with a dilation of the radial "time" direction:

$$\frac{1}{\gamma}\frac{dS_{X'}}{dt} = \frac{1}{c} \qquad \text{and} \qquad S_{X'}\frac{d\psi_{X'}}{dt} = \frac{1}{v} \qquad \Longrightarrow \qquad S_{X'} = S_1 e^{\frac{\gamma v}{c}\psi_{X'}} = S_i e^{\gamma\beta\langle v\rangle\psi_{X'}} \tag{74}$$

These graphs are large-scale projections of the polar trajectory and space axis of a moving particle's reference frame. Proper travel distances and times are contracted, preserving the relative velocity as measured in any RF. These are recognisable as time and space components of the 4-velocity $U^\mu = \gamma(c, v)$.

To illustrate and support the derivations, a relativistic particle jet P emitted by a galaxy H propagates to co-moving coordinate ψ_H, developed over several billion years in Figure 17:

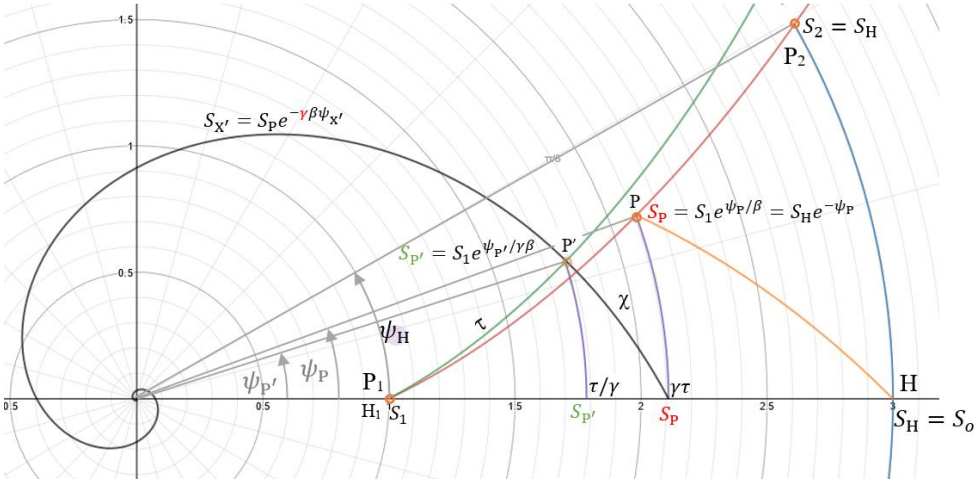

Figure 17: *Polar and* 4*-vector trajectories with corresponding dilation-contractions relative to co-moving observer* H. *The arc length along the polar trajectory from* S_1 *to* P′ *is the proper time* τ *of the moving particle. The long spiral is the corresponding polar space axis positioning* P′ *in the past relative to* P *and* H. *Local intervals* τ/γ *and* $\gamma\tau$ *provide the basis of a Lorentz-Doppler effect that arises in this geometry. This is a polar expansion of* Figure 6.

Proceed by determining ψ_P and then $\psi_{P'}$ in terms of the co-moving angle ψ_H, with rates of change determined by derivatives of the observable velocity $v = S_H\, d\psi_H/dt$, at an intersection point on the trajectory:

$$S_P = S_1 e^{\psi_P/\beta} = S_H e^{-\psi_P} \qquad \textit{past and future loci of } \mathrm{P} \textit{ developed from } S_1 \textit{ and } S_H \tag{75}$$

The visible moving coordinate ψ_P is related to the co-moving ψ_H by a form of Doppler effect:

$$S_H = S_1 e^{\psi_H/\beta} \tag{76}$$

so $$\psi_P = \frac{\psi_H}{1+\beta} \qquad \textit{spatial Doppler effect on moving and co-moving coordinates} \tag{77}$$

Continue by locating the same radius S_P along the primed polar trajectory and space axis:

$$S_P = S_1 e^{\psi_{P'}/\gamma\beta} e^{\beta\gamma\psi_{P'}} = S_H e^{-\psi_P} \qquad \textit{locus of } \mathrm{P} \textit{ from } S_1 \textit{ to } S_{P'} \textit{ then } S_P \textit{ along polar graphs} \tag{78}$$

With the previous result on the conventional trajectory, this leads to:

$$\psi_{P'} = \frac{\psi_P}{\gamma} = \frac{\psi_H}{\gamma(1+\beta)} \qquad \textit{Lorentz-Doppler coordinates} \tag{79}$$

The co-moving and contracted coordinate systems are thus related by a relativistic Doppler effect:

$$\frac{d\psi_{P'}}{dt} = \frac{d\psi_H}{dt}\frac{1}{\gamma(1+\beta)} = \frac{v}{S_H}\gamma(1-\beta) \qquad \textit{relativistic visible particle coordinate velocity} \tag{80}$$

The proper interval τ of the polar trajectory is found by integrating the 4D arc length of the dilated particle P′:

$$c^2 d\tau^2 = dr^2 + dS^2 \qquad \textit{Euclidean arc length of polar trajectory} \tag{81}$$

where $S = S_1 e^{\psi/\gamma\beta}$ extending from S_1 to the contracted angle $\psi_{P'} = \psi_P/\gamma$ (Figure 17):

so $$dr = Sd\psi = S_{P'}d\psi = S_1 e^{\psi/\gamma\beta}\, d\psi \tag{82}$$

and $$dS = S_1 \frac{1}{\gamma\beta} e^{\psi/\gamma\beta} d\psi \tag{83}$$

thus $$c d\tau = S_1\sqrt{1+(1/\gamma\beta)^2}.\, e^{\psi/\gamma\beta}\, d\psi \qquad \sqrt{1+(1/\gamma\beta)^2} = 1/\beta \tag{84}$$

$$= \frac{S_1}{\beta} e^{\psi/\gamma\beta}\, d\psi$$

or $$c\tau = S_1 \int_0^{\psi_P/\gamma} \frac{1}{\beta} e^{\psi/\gamma\beta}\, d\psi \tag{85}$$

$$= S_1\gamma\left(e^{\psi_P/\gamma^2\beta} - 1\right)$$

$$= \gamma(S_{P'} - S_1) \qquad \textit{proper interval} \qquad 86$$

where $S_{P'} = S_1 e^{(\psi_P/\gamma)/\gamma\beta} = S_H e^{-\psi_P} e^{-\gamma\beta\psi_P/\gamma} = S_H e^{-\psi_P(1+\beta)} = S_H e^{-\psi_H}$ 87

This lightlike dilation is a Euclidean length with a local or infinitesimal $\gamma = \sec\phi$ effect on universal radii (Figure 17 cf. Figure 6). This provides a Euclidean 3D distance as projections of the arc:

$$dx'_t = S_{P'}\, d\psi = S_1 e^{\psi/\gamma\beta}\, d\psi \qquad 88$$

$$x'_t = S_1\gamma\beta\left(e^{\psi_{P'}/\gamma\beta} - 1\right) \qquad 89$$

$$= \gamma\beta(S_{P'} - S_1) = \tan\phi\,(S_{P'} - S_1) \qquad 90$$

This preserves the relative velocity as observed from either H or P:

$$\frac{x'_t}{\tau} = \frac{c\gamma\beta\left(S_{P'} - S_1\right)}{\gamma(S_{P'} - S_1)} = c\beta = v \qquad \textit{preservation of relative velocity} \qquad 91$$

Cosmological Lorentz-Doppler Effect

The proper interval $c\tau$ combines with the relativistic Doppler coordinate transforms to produce a scale-modified relativistic Doppler effect:

$$c\tau = \gamma(S_{P'} - S_1) \qquad \text{(Eqn 86)}$$

$$= \gamma\left(S_H e^{-(1+\beta)\psi_P} - S_1\right)$$

$$= \gamma\left(S_H e^{-\gamma(1+\beta)\psi_{P'}} - S_1\right) \qquad 92$$

Then since γ and S_1 are fixed values for a given velocity and departure, the expansion rate of proper time is:

$$\frac{d(c\tau)}{dt} = \gamma\frac{dS_{P'}}{dt} \qquad 93$$

$$= \gamma\left[\frac{\partial S_{P'}}{\partial S_H}\frac{dS_H}{dt} + \frac{\partial S_{P'}}{\partial \psi_{P'}}\frac{d\psi_{P'}}{dt}\right]$$

$$= \gamma\left[ce^{-(1+\beta)\psi_P} - \gamma(1+\beta)S_H e^{-(1+\beta)\psi_P}\frac{c}{c}\frac{v}{S_H}\frac{1}{\gamma(1+\beta)}\right]$$

$$= \gamma c e^{-(1+\beta)\psi_P}(1-\beta) \qquad \textit{dilation of proper trajectory time} \qquad 94$$

Differentiating to the observer expansion rate $dS_H/dt = c$ produces a frequency ratio f' as a scale-modified relativistic Doppler effect, with an additional inverse Doppler effect in the index of the scale factor:

$$\frac{d(c\tau)}{dS_H} = \frac{d(c\tau)}{d(ct)} = \gamma(1-\beta)e^{-(1+\beta)\psi_P} \qquad 95$$

$$= \gamma(1-\beta)\,a^{(1+\beta)} \qquad a \textit{ the scale factor at the particle's visible coordinate } \psi_P$$

or $f' = \frac{d(c\tau)}{dS_H} = \gamma(1-\beta)a^{(1+\beta)}$ ***Cosmological Peculiar Redshift*** **96**

[III] Polar Metric, Time Scale and Horizons

An open FLRW-type *metric is derived as an equidistant projection of an open 3-sphere, with distances defined by the arc-length extent of the manifold and arc-length elements of distance on scaled light cones. Distances, velocities and intervals in the logarithmic curvature are equivalent to Lorentz transformations with a linear Pythagorean metric. The resulting scaled contraction of space corresponds to the timescale, i.e. the relative universal age on a graph of the scale factor. This compares well to the* ΛCDM *time-temperature history of the universe, with an inflection resembling the onset of acceleration.*

To align this with standard notation such as [29], a spacelike co-moving distance r is defined as a spherical great-circle arc length on an angular coordinate $\psi = r/S_o$ simultaneous with the observer. The Hubble radius $S_0 = ct_0 \equiv R_0$ in text [29] is re-aligned here as a wavelike 4-space light-distance, not a curvature, since the projected manifold** is flat. While S_0 is timelike, r is spacelike and scaled on past instances of the manifold as $r_S = ar$ where $a = S/S_0 = e^{-\psi}$ is the cosmological scale factor in a frame at that distance. The light cone distance $x = S_0(1-a)$ is derived in [I] and re-applied in the metric.

In Figure 23b) the polar metric is depicted on an open 3-sphere with a normal projective axis that follows the curvature. This differs from the orthogonal projection of the FLRW metric, Figure 23a), in that the polar metric elements are defined as observers at those distances would measure them, at covariant normals to the manifold. This removes the sine projection

** The manifold is physically independent of the embedding dimension: parallel waves of the wavefront do not intersect.

from the metric, since all measurements have the same local observer-orientation to the manifold, which is then measured as it is locally, i.e. flat. This can be modelled as a 3-sphere unrolling onto an equidistant flat 3-space, b):

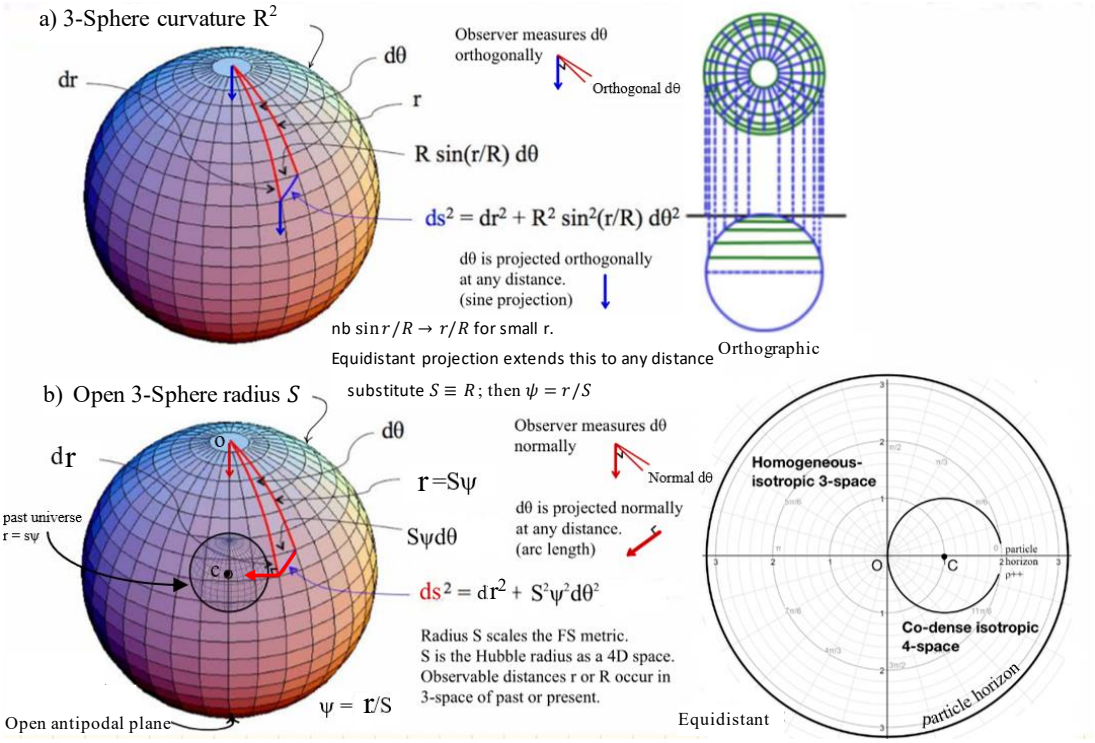

Figure 23: *Projections* a) *orthogonal in the observer's normal plane and* b) *equidistant at local normals to the manifold. Figure* a) *is the proper basis of* FLRW. *Figure* b) *instead follows the curvature, orienting continuously along the covariant basis and so flattening the space into an orthonormal definition at every point. The equidistant projection is conventionally depicted as the unrolling of a sphere onto a plane. Since this can continue past the antipode, which is just another angular coordinate, the* 3-*sphere opens to an unlimited* 3D *space wrapped around a* π-*compactified* 4D *manifold with co-dense horizons. The radius* $S = aS_o$ *is linked to the expansion scale factor.* Images courtesy Whittle, M; ESRI; Desmos.

The azimuthal-equidistant projection has distorting effects that are smoothed in a homogeneous cosmos. For the resulting 3-space to be isotropic-homogeneous, orienting the 3-space onto the 4-space must produce a density crisis at the antipode. This is identified with the singularity in visible past time (cf. Figure 19 [II]) due to densification towards the Big Bang. Observable and visible spaces are thus correlated in density distribution, with co-dense singularities. This geometric compactification can be matched to a conformal integral [III, i.e. this section], which guarantees similarities in energy density, analysed in observable [II] and visible spaces [IV].

The metric has spherical symmetries and scaled expansion and as such can be derived in terms of an FLRW metric with a locally orthogonal definition of light distance on scaled radial elements dr_S on arcs of the co-moving coordinate:

$$dx = cdt = dr_S = Sd\psi = ctd\psi = aS_o d\psi = adr = e^{-\psi}dr \qquad \text{(Eqn 32)}$$

hence $x = S_o(1 - e^{-\psi}) = S_o - S = ct_o - ct = c\Delta t_o = S_k(r)$ (Eqns 39 – 42)

Past-scaled distance and time intervals corresponding to the scaled radial arc-distance r_S emerge from scale-similarities:

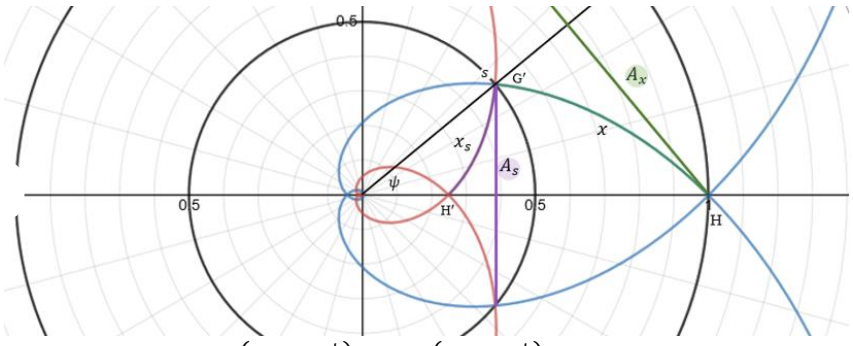

$$x_s = ax = S(1 - e^{-\psi}) = aS_0(1 - e^{-\psi}) \qquad 168$$

and $dt = adt_0$ (Eqn 52)

An observable distance, the spacelike radial distance in an earlier epoch, has the same infinitesimal definition as dx but a time-constant scale factor at co-moving distances:

$$dr_S = dx = Sd\psi$$

$$r_S = S\psi = ar = e^{-\psi}S_0\psi \qquad \text{(Eqn 30)}$$

Here $S\psi$ is monotonic and unlimited, i.e. open angular coordinates up to and beyond $\psi > \pi$. This is the observable metric, which is not empirical but transforms in co-moving coordinates onto the presently visible lightcone. The visible metric is a scaled Lorentz-signature with the derived light-distance law on present and past elements:

$$\begin{aligned} ds^2 &= -c^2dt^2 + a(t)^2(dr^2 + S_\kappa(r)^2 d\Omega^2) \\ &= -a(t)^2c^2dt_0^2 + dx^2 + a(t)^2 S_0^2\left(1 - e^{-\psi}\right)^2 d\Omega^2 \\ &= -dS^2 + dx^2 + x_s^2 d\Omega^2 \qquad \textit{a flat space in this projection} \end{aligned} \qquad 169$$

On a null lightcone $ds^2 = 0$ and $d\Omega^2 = 0$:

$$\frac{d\psi}{dt} = \pm\frac{ic}{s} = \pm\frac{i}{t} \qquad \textit{as per [I] with imaginary conjugate times} \qquad 170$$

Here $dt = ad\,t_0$ is a redshifted interval and $ax = x_s$ is the distance as measured by a past observer at that scale with reference to the t_0 observer. The scaled x_s corresponds to the distance of inverse-square effects on magnitude and gravitation, explored as a Friedmann solution in [IV]. For comparison, conventional FLRW spherical coordinates $d\Omega^2$ follow alternative possible curvatures with the specific present values of r and R_0:

$$S_\kappa \equiv x = \begin{Bmatrix} R_0 \sin(r/R_0) \\ R_0(r/R_0) \\ R_0 \sinh(r/R_0) \end{Bmatrix} \begin{matrix} \kappa = +1 \\ \kappa = 0 \\ \kappa = -1 \end{matrix} \qquad \textit{where } R_0 \equiv S_o \textit{ is GR radius of curvature [29 Eqn 3.18]}$$

nb $$\frac{x}{S_0} = \frac{v_x}{c} = \beta_x = \left(1 - e^{-\psi}\right) = az = \sin\phi_x \to \sin\psi \to \psi \textit{ as } \psi \to 0 \qquad 171$$

Eqn 169 contains an implicit γ_x due to the recurring Huygens-Lorentz structure of the metric (Figure 24 below):

$$ds^2 = -c^2d\tau^2 = -c^2dt^2 + dx^2 \qquad \text{Eqn 169 } \textit{on radial trajectory } d\Omega = 0$$

i.e. $$c^2d\tau^2 + dx^2 = c^2dt^2 \qquad \textit{Pythagorean cosmological metric} \qquad 172$$

As before [I], these Lorentz signature metric components can be plotted as right-triangles with dynamic wavelet constructions (Figure 24). The cosines and sines are $\sec\phi_x = \gamma_x$ and $\sin\phi_x = x/S_o = v_x/c$. This is consistent with a global flat Minkowski space of distant inertial reference frames at relative recession velocities.

This does not extend the metric beyond the frame. Distant and local reference frames are both as measured at that location, i.e. the distant RF and the lab observer measure the time element by a local observer's clock and the distance element by the scaling at that time. Recession is scaled to distance so that $dx = v_x dt \le cdt$.

The recession factor γ_x derives as per any flat metric and can be recognized again as a $\sec\phi$ projection:

$$\begin{aligned} c^2d\tau^2 &= c^2dt^2 - dx^2 \\ &= c^2dt^2\left(1 - \frac{v_x^2}{c^2}\right) = dS^2\left(1 - \frac{x^2}{S_0^2}\right) \\ &= c^2\frac{a^2}{\gamma_x^2}dt_o^2 = \frac{a^2}{\gamma_x^2}dS_0^2 \qquad \text{nb} \quad d\tau = \frac{a}{\gamma_x}dt_o = \frac{dt}{\gamma_x} \\ &= \cos^2\phi_x\, dS^2 \end{aligned} \qquad 173$$

Other projection effects follow. In particular, space contraction at an observed distance must involve a contraction of co-moving coordinate at that distance. The following metric analysis is dominated by the result $d\psi' = d\psi/\gamma_x$.

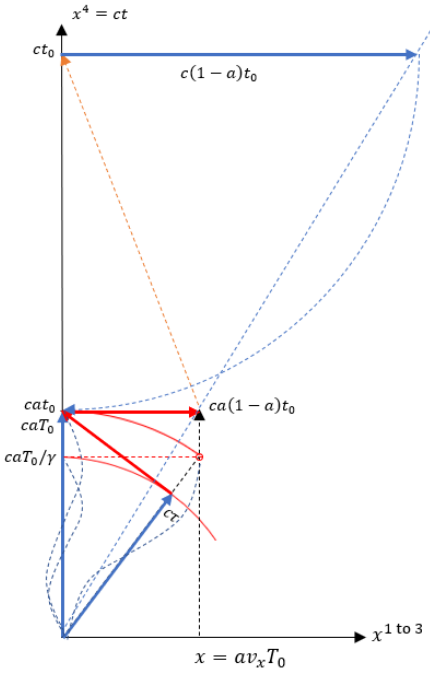

Assuming Lorentz effects due to recession, motion at a visible distance is dilated. The total distance a co-moving particle could move at $v_x = c(1-a)$ to age $t = at_0$ is $x = ca(1-a)\,t_0$. The distance it could move in one cycle is $X = c(1-a)T_0$ scaled in past time to $x = av_xT_0$.

There is a phase number $n = t_0/T_0$ such that $ct_0 = cnT_0$ and the observed particle is at $ct = act_0 = acnT_0$. The resulting frequency is not quite a Doppler effect:

Phase change $\Delta\varphi = \frac{an}{\gamma}$ Time interval $\Delta t = t_0$

Frequency $f_{obs} = \frac{\Delta\varphi}{\Delta t} = \frac{an}{\gamma_x t_0} = \frac{a}{\gamma_x T_0} = \frac{a}{\gamma_x}f_s = \frac{1-\beta_x}{\gamma_x}f_s$

This is an advance on dilation by a local 3-spatial Doppler effect $f_{obs} = \gamma_x(1-\beta)f_s$ the larger effect here due to the scaling of distance by expansion i.e. this is a cosmological Lorentz-Doppler effect.

Figure 24: *The maximally extended metric* (Eqn 169) *has the same spherical Huygens symmetries as the particle and gravitation models derived in* [I]. *In particular the integration of distance by general relativistic methods must allow for contraction of co-moving coordinates, which becomes a conformal distance calculation on a compactified polar universe.*

Time evolves in the same proportion as phase i.e. $\tau = \frac{a}{\gamma}T_0$. Then since the scaled epoch $t = at_0$ is only a phase multiple of scaled-dilated intervals, universal ages are scaled-dilated:

$$\tau = \frac{a}{\gamma}t_0$$

The co-moving particle has relative energies in the period of the phase wave, shown here as

$$T' = \frac{aT_0}{\gamma} = \frac{ah}{\gamma mc^2}$$

such that $E = hf' = \gamma mc^2/a \rightarrow \gamma mc^2 z$

as phase/frequency (energy) and wavelength (momentum) are contracted. z is a larger effect than γ: $z \sim 1100$ when $\gamma \sim 24$.

The resulting redshift is canonical:

$f_{obs} = cycles/time$

$cycles = f_{source}\tau = f_s a t_0/\gamma_x$ i.e all cycles of an inertial receding particle in the timescale of that epoch…

$time = t_0$ …occurring in the universal time at observation.

Hence $f_{obs} = f_s a/\gamma_x$

But $f_{source} = \gamma f_0$ energy of source is $hf_{source} = \gamma_x mc^2$

So $f_{obs} = f_0 a$ frequency scaled from rest frequency $hf_0 = mc^2$

And $z = \frac{f_0}{f_{obs}} - 1 = a^{-1} - 1$

This analysis shows that there are energy scaling factors "hidden" in the redshift, i.e. inertially receding particles are energetic but dilated in our view so that only the scale factor remains. The energy analysis in II follows this same point in a classical methodology and finds good agreement with observed "dark" energy densities.

Recession Lorentz Factor

An object such as a galaxy seen at significant recession can be thought of as time-dilated by cosmological redshift. It follows that the total measured time interval to any distance can be integrated as a sum of progressively dilated elements of time at each continuous distance.

Assuming spacetime symmetries, total distances to any coordinate would also be an integral sum of recession-contracted distance elements. There is in fact only one other way to determine distance in a Riemannian geometry. The result is a natural compactification towards a finite conformal horizon.

A Lorentz-FitzGerald factor γ_x for this effect is constructed as a function of the derived light-distance law:

$$v_x = c\left(1 - e^{-\psi}\right) \quad \text{(Eqn 44)}$$

$$v_x/c = x/S_o = \beta_x = 1 - e^{-\psi} \quad \text{(Eqn 67)}$$

The squared β_x factor then provides a Lorentz-FitzGerald γ_x factor:

$$\beta_x^2 = 1 - 2e^{-\psi} + e^{-2\psi} \quad 176$$

i.e. $\gamma_x^{-1} = \sqrt{1 - \beta_x^2} = \sqrt{1 - (1 - 2e^{-\psi} + e^{-2\psi})}$

or $\gamma_x^{-1} = \sqrt{2e^{-\psi} - e^{-2\psi}} = \sqrt{2a - a^2}$ *cosmological Lorentz-FitzGerald factor* 177

This is a reformulation of the Lorentz-FitzGerald factor for recession as a relative velocity. This governs the scale of space contraction and time dilation due to recession. In effect this is a modified scale factor.

Real solutions to this square root exist only between $a = 0$ and $a = 2$. In that range the proper timescale is contracted by recession relative to the present:

$$\tau = at_0/\gamma_x = t_o a\sqrt{2a - a^2} \underset{a\rightarrow 0}{\longrightarrow} t_o a^{3/2}\sqrt{2} \underset{a\rightarrow 2}{\longrightarrow} 0 \qquad \textit{Recession Timescale}$$

Normalizing $t_0 = S_0 = c = 1$, the proper timescale becomes a product of the linear scale factor and the circular contraction factor. The scale factor appears to decelerate then accelerate:

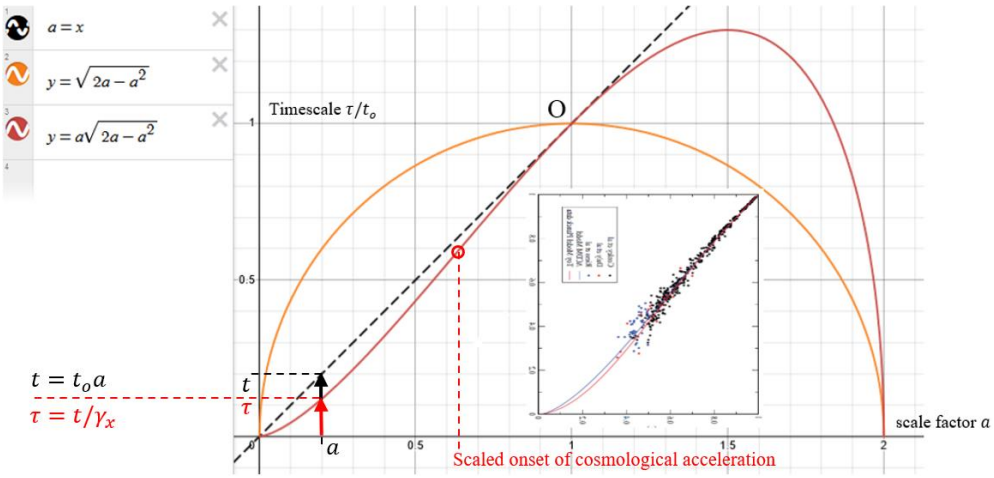

Spherical Huygens geometry of the relativistic scale-factored cosmos, with circular-linear scales and non-linear relativistic corrections. Scale factors greater than one are future time. The observer is at O, *scale factor* $a = 1$. *A dilated timescale is shown at* $a = 0.2$ *Inset:* Ringemacher and Mead, 2015 *showing a match to the apparent* ΛCDM *cosmic acceleration, explained as a scale effect.*

The scale factor is plotted first as a linear function of expanding space or time, generically labelled x, then as the inverse dilation gamma generically labelled y, and lastly as a relative timescale factor which is scaled by expansion *and* dilated by recession. The combination of both effects also occurs in standard-model measurements that suggest an acceleration (inset). This is not an acceleration, but a scaling effect or contracted scale factor giving a dilated timescale $a' = a/\gamma_x = \tau/t_0$. Dilation of cosmological time has recently been confirmed†† in quasar studies by Lewis and Brewer at Sydney University.

The polar model predicts a slightly smaller scale factor than ΛCDM for any timescale, which is consistent with a model of zero acceleration compared to a positive acceleration. See Eqns 235+ for this parameterisation of ΛCDM. The comparison tends to question the nature of the acceleration, since a zero-acceleration model has almost exactly the same inflection. It will help to compare the polar to a zero-acceleration variant of FLRW.

Conformal Event Horizon

In Figure 26, scale factors $a > 1$ up to $a = 2$ can be identified with negative co-moving coordinates, i.e. future coordinates corresponding to future observers G who may see the state of the present observer H along their past light cone. Calculations of scale factor and coordinate at distances seen from future frames are consistent with the present:

$$a = e^{-\psi} = 2 \quad : \quad \psi = -\ln(2) = -0.693 \text{ radians} \tag{191}$$

$$x = S_o\left(1 - e^{-(-\ln 2)}\right) = S_o(1 - 2) = -S_o \tag{192}$$

In the limit future reference frame or event horizon at $a = 2$, the angular coordinate to the present is a positive value of the same magnitude at a scale factor of 0.5, i.e. as seen from a radius twice the present size:

$$a = e^{-\psi} = 0.5 \quad : \quad \psi = -\ln(0.5) = 0.693 \text{ radians} \tag{193}$$

$$x = S_2\left(1 - e^{-(-\ln 0.5)}\right) = 2S_o(1 - 0.5) = S_o = \tfrac{1}{2}S_2 \tag{194}$$

The same distance in either direction, is yet only half the proper particle horizon distance as seen from the future RF, because the particle horizon distance increases with scale. The present recession velocity from the future RF is consistent with that and is fixed by the speed of light:

$$v_x = c(1 - a) = c(1 - 0.5) = c/2 \tag{195}$$

The collapsing time scale beyond $a > 1.5$ can only be understood in relative terms. There is a finite future age of the universe from the observer's frame of reference, but that finite age limit expands as the universe expands with constant real lightspeed. The future limit or event horizon at $a = 2$ recedes as the space at that scale recedes.

Redshift and Particle Horizon

A de Broglie particle model, previously related to the Huygens-Lorentz metric [I, Eqn 16], clarifies the redshift implications of a compactified horizon and associated timescale.

A particle in relative recession is assumed to follow equivalent wavelength-momentum laws as in relative motion, where both the wavelength and the interval are modified by the scale recession factor. A particle's rest wavelength and interval (assuming a free particle, for a direct solution), as observed at a great distance by scattering, are scaled and contracted in the metric.

†† Lewis, G.F and Brewer, B.J. 2023. "Detection of the cosmological time dilation of high-redshift quasars" *Nature Astronomy*. https://doi.org/10.1038/s41550-023-02029-2

A particle at rest at great distance is observed in its rest state at that distance and scale, since it is co-moving, so the observable redshift is scaled and not contracted by local motion, as per the standard model. So obviously

$$T_0 = aT_{obs} = T_{obs}\, e^{-\psi} \qquad 196$$

Here T_{obs} is the observed period in the present, which is redshifted by scale factor a from the rest value T_0 for an inertial particle:

$$T = \frac{T_0}{\gamma_x} = \frac{h}{\gamma_x mc^2} = \frac{aT_{obs}}{\gamma_x} \qquad 197$$

$$\lambda = \frac{h}{\gamma_x m v_x} = \frac{cT_0}{\gamma_x \beta_x} = \frac{a}{\gamma_x}\frac{cT_{obs}}{\beta_x} \qquad \text{nb} \qquad \frac{a}{\gamma_x}T_{obs} = \frac{v}{c^2}\lambda \qquad \textit{scaled de Broglie } \mathrm{M}^4 \textit{ wavelength} \qquad 198$$

To the present observer, the dilated cosmological time interval to a scattering event can be integrated [III, i.e. this section] with the recession factor to account for the dilation effects of co-moving expansion, which must occur in a theory with corresponding relative energies. The timescale adds up the dilated proper time of virtual particles at continuous distances to the most distant real particle, and provides a thermal history by the corresponding timescale power law:

$$\tau = \frac{a}{\gamma_x}t_{obs} = \frac{a}{\gamma_x}t_o \qquad 199$$

Here t_o is the present observer's measurable age of the universe and τ is the corresponding scaled age at a co-moving coordinate $\psi = -\ln a$. Particles in high redshift near the CMB, approximating the particle horizon (eg Figure 25), are conformally contracted onto the horizon. Contact by entanglement of virtual particles throughout spacetime would tend to draw particles onto the horizon, suggesting a mechanism within this theory for the holographic principle to operate.

This is speculative, however it derives consistently from the same first principles as [I] and is of significant interest as a tractable theory that accesses both the particle and event horizons in similar and symmetrical terms, consistent with expansion redshift theory and equilibrium thermodynamics.

Conformal Extended Spacetime

The recession Lorentz factor γ_x is a function of distance in co-moving coordinates and can be analysed for conformal effects on the global model. A maximally symmetric extended spacetime is the result. There are other ways of framing this with natural symmetries.

In the observer's view of a receding frame, an infinitesimal proper lookback interval $dt = adt_o$ (dt_o a local moment of observation) may be considered to be Lorentz-dilated $dt' = \gamma_x dt$ as per the standard framing of dilated time. Similarly an element of proper distance x is contracted $dx' = dx/\gamma_x = cdt/\gamma_x = cdt'/\gamma_x^2$:

$$dt' = \gamma_x dt = \gamma_x a dt_o \qquad 205$$

$$dx' = \frac{dx}{\gamma_x} = \frac{aS_o d\psi}{\gamma_x} \qquad \textit{contraction inclusive of the scale factor} \qquad 206$$

The element dt derives from elements of distance dx equivalent to a scaled trajectory at lightspeed:

$$dx = Sd\psi = cdt \quad ; \quad dt = \frac{S}{c}d\psi \qquad 207$$

i.e. $$dt' = \gamma_x \frac{S}{c}d\psi = \gamma_x t d\psi = \gamma_x a t_o d\psi \qquad \textit{dilation inclusive of the scale factor} \qquad 208$$

Given the association of these relativistic effects with the Huygens-Lorentz model, it is expected that angular expressions of the scale factor due to recession will become significant:

$$\phi_x = \sin^{-1}(v_x/c) = \sin^{-1}(x_o/S_o) = \sin^{-1}\left(1 - e^{-\psi}\right) \quad \Rightarrow \quad \cos(\phi_x) = 1/\gamma_x \qquad 209$$

Cosmological Time Dilation

Dilation of intervals at great distances due to recession velocity are evaluated. Time dilations of distant recession frames are assumed to accumulate with coordinate:

Given $$dt' = \gamma_x \frac{S}{c}d\psi \qquad \text{(Eqn 208)}$$

i.e. $$dt' = \frac{1}{\sqrt{2e^{-\psi} - e^{-2\psi}}}\frac{S_o e^{-\psi}}{c}d\psi \qquad 210$$

where $\frac{S_o}{c} = \frac{1}{H_o} = t_o$ i.e. the present age of the universe as a co-moving universal value.

$$t' = t_o \int_0^{\psi} \frac{e^{-\psi}}{\sqrt{2e^{-\psi} - e^{-2\psi}}}d\psi \qquad 211$$

This has a straightforward trigonometric solution:

$$t' = t_o \sin^{-1}\left(1 - e^{-\psi}\right) \qquad \textit{dilated lookback time} \qquad 212$$

An expected angular function $\phi_x = \sin^{-1}(1 - a)$ emerges from the analysis. At small distances, $\phi_x \to \psi \to 0$, while at large distances, $\phi_x \to \pi/2$ as $\psi \to \infty$.

The lookback time dilates to a square geometry relative to a proper time interval in the past:

$$\frac{t'}{t} = \frac{t_o \sin^{-1}(1 - e^{-\psi})}{t_o - t} = \frac{\sin^{-1}(1-a)}{1-a} = \frac{\phi_x}{\beta_x} = 1 \to \frac{\pi}{2} \qquad 213$$

Taking ψ to large values, dilated time converges to a fixed maximum Lorentz-dilated time that evolves with universal age and forms a right angle at universal time:

$$t'_{\max} = t_o \sin^{-1}(1 - 0) = \frac{\pi t_o}{2} \qquad \textit{maximum dilated lookback time} \qquad 214$$

This is interpreted as a dilated lookback time in the observer's reference frame. A shorter proper time has passed within a distant reference frame compared to the observer's laboratory time measuring that distant era.

Cosmological Space Contraction

A correlated scale Lorentz contraction is derived for visible distance based on equal elements of proper length at any co-moving coordinate:

$$S d\psi = c dt \qquad \text{at any } \psi \qquad 215$$

A contracted distance element can then be integrated to a universal contracted distance:

$$dx' = \frac{S d\psi}{\gamma_x} = S_o e^{-\psi}\sqrt{2e^{-\psi} - e^{-2\psi}}\, d\psi \qquad \text{Contracted distance element} \qquad 216$$

$$x' = \int_0^{\psi} dx' = S_o \int_0^{\psi} e^{-\psi}\sqrt{2e^{-\psi} - e^{-2\psi}}\, d\psi$$

$$= \frac{S_o}{4}\left[2\sin^{-1}\left(1 - e^{-\psi}\right) + \sin\left(2\sin^{-1}\left(1 - e^{-\psi}\right)\right)\right] \qquad \text{contracted lookback distance} \qquad 217$$

Note that since $e^{-\psi} = (1 - v_x/c) = a$: (Eqns 67, 36)

then $$x' = \frac{S_o}{4}\left[2\sin^{-1}\left(1 - e^{-\psi}\right) + \sin\left(2\sin^{-1}\left(1 - e^{-\psi}\right)\right)\right]$$

$$= \frac{S_o}{4}\left[2\sin^{-1}(\beta_x) + \sin\left(2\sin^{-1}(\beta_x)\right)\right]$$

$$= \frac{S_o}{4}\left[2\phi_x + \sin(2\phi_x)\right] \qquad 218$$

i.e. the contracted spacetime distance can be evaluated in terms of a number of related parameters: Co-moving coordinate $\psi = r/S$; scale factor $a = S/S_o$; or recession velocity ratio $\beta_x = v_x/c = x/S_o = \sin\phi_x$.

The inverse sine identity of time dilation provides a relationship between contracted distance and dilated time variables:

$$\sin^{-1}\left(1 - e^{-\psi}\right) = \frac{t'}{t_o} \qquad 219$$

so $$x' = \frac{S_o}{4}\left[2\sin^{-1}\left(1 - e^{-\psi}\right) + \sin\left(2\sin^{-1}\left(1 - e^{-\psi}\right)\right)\right]$$

$$= \frac{S_o}{4}\left[2\frac{t'}{t_o} + \sin\left(2\frac{t'}{t_o}\right)\right] \qquad 220$$

At small intervals the sine function and its argument converge on equal, so the interval-distance to a near coordinate reduces to $t' = t = \Delta t$:

$$x' = \frac{S_o}{4}\left[2\frac{\Delta t}{t_o} + 2\frac{\Delta t}{t_o}\right]$$

$$= S_o\frac{\Delta t}{t_o} = S_o\phi_x \sim S_o\psi$$

$$= ct_o\frac{\Delta t}{t_o}$$

$$= c\Delta t \qquad 221$$

Again taking ψ to large values, equivalent to large recession velocities, Eqn 217 converges to a maximum Lorentz-contracted (compactified) distance in the visible universe:

$$x'_{max} = \frac{S_o}{4}\left[2\sin^{-1}(1) + \sin\left(2\sin^{-1}(1)\right)\right]$$

$$= \frac{S_o}{4}\left[\pi + 0\right]$$

$$= \frac{\pi S_o}{4} \qquad \text{maximum contracted lookback distance} \qquad 222$$

This is a relativistic contraction of proper space at the maximum visible distance. As with conventional length contraction, the effect is not visible to the observer since it subtends no angle on the sky and cannot be compared by measurement to a given stationary (observer) length [17, 18].

The relativistic distance x' is the Lorentz-contracted distance to the same set of presently visible proper distances in spacetime, at correspondingly dilated times for events at that distance. The convergence with Epstein trigonometry is suggestive of internal consistency in this cosmology since [I].

These same formulae can be derived for distance-proportional recession in Cartesian coordinates, indicating that this is a general property of flat spacetime. The construction produces another circular model, with projection arcs of contracted-dilated spacetime (Figure 29) including proper $1 - a$ and timescale a/γ_x functions. The rotation of space to time with other complex effects includes a wake as in [I] and is reminiscent of the concept of imaginary time [36].

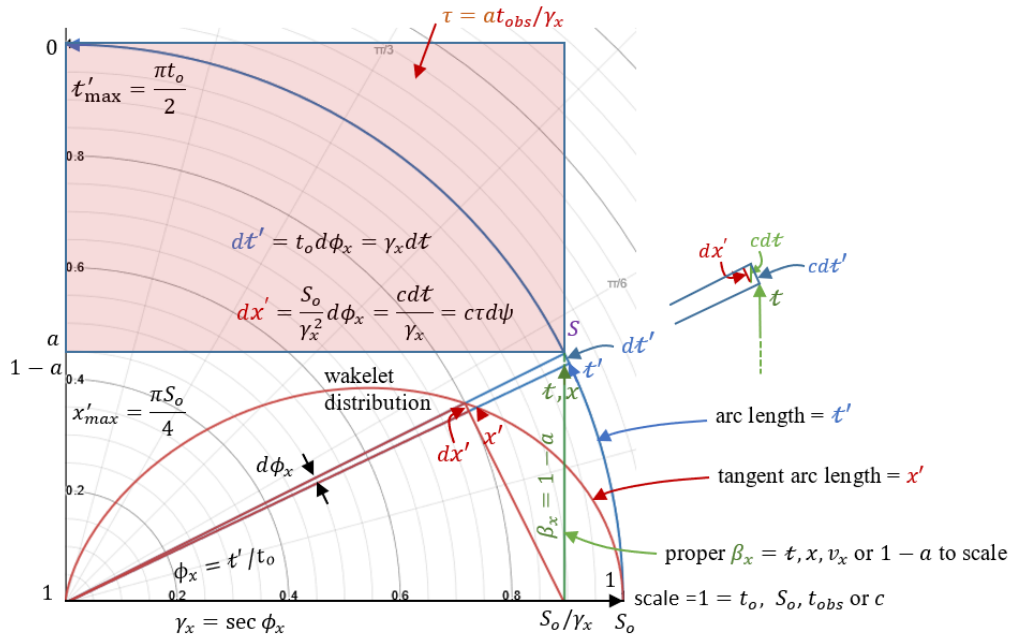

Figure 29: Conformal spacetime looking in any outward direction with recession contraction-dilation effects at distance. Dilated and contracted intervals are integrated along arc elements on proper or contracted radii. Lookback times, distances and recessions are plotted on the same scale as the observer's linear time t_o, or Hubble radius S_o, or the speed of light.

A further condition on this analysis is that visible and observable manifolds should be related by a conformal scale factor near a value of 3+, that is the Hubble radius is scaled by integration of distance to a conformal $r_{max} = \pi S_o$. In fact the integral of the cosmological Lorentz contraction factor over all real solutions for ψ is exactly π:

$$\int_{-\ln(2)}^{\infty} \sqrt{2e^{-\psi} - e^{-2\psi}}\, d\psi = \pi \qquad 223$$

Dilated Recession

The scaled recession factor a/γ_x is the timescale against which distant co-moving particles are at rest. This implies dilatory effects that produce measurable deviations from the distance-velocity law, with predictable effects on redshift and magnitude.

To take the idea of relative recession seriously, we require that all of the normal effects of a boost in special relativity, for example a recession Lorentz-Doppler effect, should apply. Cosmological redshift is conventionally restricted to the scale factor, simply the past size of the GR universe, and does not count the recession as a boost in the redshift.

The scale factor in the proposed theory does not contradict this when it is identified [I] with the Doppler term of a Lorentz effect:

Since $v_x = c(1-a)$ (Eqn 44)

$$a = \frac{\lambda_s}{\lambda_o} = (1 - \beta_x) \qquad 200$$

This can be construed as a Lorentz-Doppler frequency redshift lacking only the Lorentz factor:

$$z = \frac{\lambda_o}{\lambda_s} - 1 = \frac{f_s}{f_o} - 1 = \sqrt{\frac{1+\beta_s}{1-\beta_s}} - 1 = \gamma_s(1+\beta_s) - 1 \qquad 201$$

i.e $a = \frac{1}{\gamma_s(1+\beta_s)} = \gamma_s(1-\beta_s)$ *correspondence to SR redshift* 202

SR may be correct both locally and at cosmological scales, where homogeneous gravitational fields develop a tideless background. The correspondence is explored further with a general relativistic treatment as follows.

Co-moving Observable Universe: Conformal Scale Factor and Horizons

The size of the observable universe can be derived from the metric. In the standard model, with no special-relativistic contraction at the cosmological scale, co-moving radius depends only on scale factor:

$$\chi = \int_0^{t_o} \frac{cdt}{a(t)} \qquad \text{in simplest possible terms} \qquad 224$$

The formal GR construction of recession velocity is

$$v_{rec} = \dot{a}(z) \int_0^z \frac{c dz'}{H(z')} \qquad [37 \text{ Eqn } 3]$$

The analyses of scale factor and Hubble constant in [I] allow this to be calculated in visible or observable frames. In the visible, the Hubble value is a constant throughout space while redshift scales the rate factor $\dot{a} = \dot{S}/S_o$:

Vis: $v_{vis} = c\frac{\dot{S}(z)}{S_o}\int_0^z \frac{dz'}{H(z')}$ $\dot{S}(z) = ac = \frac{dS}{dS_o}\frac{dS_o}{dt}$ in visible frame ($\dot{S} = c$ in observable) 225

$= c\frac{ac}{ct_o}\int_0^z \frac{dz'}{H_o}$ $H = H_o$ constant *throughout presently visible spacetime*

… $v_{vis} = \frac{ac}{t_o}\int_0^z t_o dz'$ $\frac{1}{H_o} = t_o$

$= acz = ac(a^{-1} - 1) = c(1 - a)$ as derived [I] and reapplied [III] 226

cf $v_x = c(1 - e^{-\psi}) = H_o x$ and $x_o = S_o(1 - e^{-\psi})$ RE velocity and distance

Conversely in the observable frame, *H* varies with distance while all Hubble radii expand at light speed:

Obs: $v_{obs} = c\frac{\dot{s}(t)}{S_o}\int_0^z \frac{\pm dz'}{H(z')}$ $\dot{s}(t) = c$ *(observable)* 227

$= c\frac{c}{ct_o}\int_0^{S(z)} \frac{S(z')}{c}\frac{dz'}{ds}dS$ *switching integral and limits to S, with* $H = \frac{c}{S}$

$= \frac{1}{t_o}\int_1^{a(z)} S(a')\frac{dz'}{da'}da'$ *…and to limit* $a(0) = 1$ *… c cancels*

$= \frac{1}{t_o}\int_1^{a(z)} a' S_o \frac{-1}{a'^2}da'$ $S = aS_o\ ;\ z = a^{-1} - 1 \rightarrow \frac{dz}{da} = -a^{-2}$

$= \frac{ct_o}{t_o}\int_1^{a(z)} \frac{-1}{a'}da'$ $S_o = ct_o$ *… c returns*

$= c\int_0^{\psi(z)} d\psi'$ $a = e^{-\psi}\ ;\ \frac{da}{d\psi} = -e^{-\psi} = -a$

$= c\psi'$ *as derived on an observable arc length* 228

This is consistent with an arc-length observable distance and c-valued expansion velocity:

$R = S\psi$ $S = ct$ $\frac{dR}{dt} = \frac{\partial R}{\partial S}\frac{dS}{dt} = \psi c$ *superluminal recession* (Eqn 111)

Relativistic contraction effects due to recession velocity are an additional effect on the conformal integration. Using the conventional GR integration of the scaled co-moving Hubble radius, the integrand and limits can be switched. The definite integral sums from past time to now. An indefinite integral looking back from now to the particle horizon beyond $z = 1100$ would reverse and drop the limits by adding an integration constant:

$\chi = \int_0^{t_o} \frac{cdt'}{a(t')}$ 229

$= \int_{S_o}^0 \frac{dx'}{a(x')}$ $dx' = \frac{dx}{\gamma} = S_o e^{-\psi}\frac{d\psi}{\gamma}$ *limits switch to distance:* $x_{max} = S_o$

$= \int_\infty^0 \frac{S_o e^{-\psi}}{\gamma}\frac{d\psi}{a(\psi)}$ $a(\psi) = e^{-\psi}$; $1/\gamma = \sqrt{2e^{-\psi} - e^{-2\psi}}$ *limits switch to coordinate*

$= S_o\int_0^\infty \sqrt{2e^{-\psi} - e^{-2\psi}}d\psi$ *reverse limits to look outward in distance, recession and redshift*

$= S_o\int \sqrt{2e^{-\psi} - e^{-2\psi}}d\psi$ *drop limits to plot recession effects as a function of coordinate* 230

i.e. $\chi = S_o[\sin^{-1}(1 - e^{-\psi}) - \sqrt{2e^{-\psi} - e^{-2\psi}} + C']$ 231

$= 0\ @\ \psi = 0$ so $C' = 1$

and $\chi' = \pi S_o\ @\ \psi = \infty$ $\rightarrow$ $C' = \frac{\pi}{2}$

C' is a dilating integration constant, interpreted as the effect of an affine connection [38] varying along the null integral. An immediate candidate substitution is the ratio of dilated to proper lookback time in Eqn 213: This function of coordinate is unity in proper terms at any coordinate, as measured by observers at that distance, and hence differentiates to zero in the global frame while dilating to $\pi/2$ in the local oberver's RF:

$\frac{t'}{t} = \frac{\sin^{-1}(1-e^{-\psi})}{1-e^{-\psi}} = \frac{\phi_x}{\beta_x}$ *dilating integration constant* $C' = \frac{t'}{t} = 1 \rightarrow \frac{\pi}{2}$ (Eqn 213)

↓

$v_{rec} = c\left[\sin^{-1}(1 - e^{-\psi}) - \sqrt{2e^{-\psi} - e^{-2\psi}} + \frac{\sin^{-1}(1-e^{-\psi})}{1-e^{-\psi}}\right]$ (Eqn 231)

$= c\left[\sin^{-1}(\beta_x)\left[1 + \frac{1}{1-e^{-\psi}}\right] - \frac{1}{\gamma_x}\right]$

$= c\left[\phi_x\left[\frac{2-e^{-\psi}}{\beta_x}\right] - \frac{1}{\gamma_x}\right]$

$= c\left[\frac{\phi_x}{\beta_x}\frac{[2e^{-\psi} - e^{-2\psi}]}{e^{-\psi}} - \frac{1}{\gamma_x}\right]$

…$= c\left[\frac{\phi_x}{\beta_x}\frac{1}{\gamma_x^2 a} - \frac{1}{\gamma_x}\right]$ *these various functional forms are illustrative…* 232

$= c\left[\frac{\phi_x}{\gamma_x\beta_x}\frac{a^{-1}}{\gamma_x} - \frac{1}{\gamma_x}\right]$

$v_{rec} = \frac{c}{\gamma_x}\left[\frac{\phi_x}{tan\phi_x}a^{-1} - 1\right]$ *…and related to the redshift* 233

$\rightarrow cz\ @\ \psi \rightarrow 0$

$\rightarrow \pi c\ @\ \beta_x \rightarrow 1$ *proof of concept: convergence to standard model at both extremes* 234

The general relativistic analysis of visible and observable recession develops consistent results, both internally and by comparison to standard model. This can now be compared to the complete functional form of ΛCDM recession velocity (Figures 30 and 31).

ΛCDM: Integration of Energy Densities for Observable Radius and Recession Velocity.

ΛCDM is paramaterised on energy densities measured by gravitational lensing and by redshift and magnitude of standard candles. The copy-dated best-fit model and data [49] are:

$$H(a) = H_o\sqrt{\Omega_{R,0}a^{-4} + \Omega_{M,0}a^{-3} + \Omega_{K,0}a^{-2} + \Omega_{\Lambda,0}} \qquad \textit{past Hubble value} \qquad 235$$

$$t_o = \frac{1}{H_o}\int_0^1 \frac{a.da}{\sqrt{\Omega_{R,0}+\Omega_{M,0}a+\Omega_{K,0}a^2+\Omega_{\Lambda,0}a^4}} \qquad \textit{present universal age} \qquad 236$$

also $$\chi = \frac{c}{H_o}\int_0^1 \frac{da}{\sqrt{\Omega_{R,0}+\Omega_{M,0}a+\Omega_{K,0}a^2+\Omega_{\Lambda,0}a^4}} \qquad \textit{co-moving radius} \qquad 237$$

$$v_{rec} = H_o\chi = c\int_0^1 \frac{da}{\sqrt{\Omega_{R,0}+\Omega_{M,0}a+\Omega_{K,0}a^2+\Omega_{\Lambda,0}a^4}} \qquad \textit{observable recession velocity} \qquad 238$$

with

$\Omega_{R,0} = 9.24 \times 10^{-5}$ radiation density

$\Omega_{M,0} = 0.3147$ matter density

$\Omega_{\Lambda,0} = 0.6842$ dark energy density

hence $\Omega_{K,0} = 0.001$ residual curvature ~ 0 : flat

The recombination scale factor $a_r = 2.725/3000 = 9.083 \times 10^{-3}$ is used as an initial condition for numerical analysis of these quantities. The model can be integrated to any time past or present. The resulting universal age is compared to concordance model analysis for verification of this first-order tabular integration method:

$$t_o = 13.804 \times 10^9 \text{ years} \quad \text{cf} \quad t_o = 13.797 \times 10^9 \text{ years [9] (0.05\%)} \qquad 239$$

The co-moving radius and observable velocity are governed by a conformal scale factor:

$$v_{\Lambda M} = H_o\chi = c\int_{a_r}^1 \frac{da}{\sqrt{\Omega_{R,0}+\Omega_{M,0}a+\Omega_{K,0}a^2+\Omega_{\Lambda,0}a^4}} \to c \times 3.1456 \quad \text{by the same analysis} \qquad \text{(Eqn 238)}$$

This can be compared with the tractable integrated result of the previous section:

$$v_{RE} = \frac{c}{\gamma}\left[\frac{\sin^{-1}(1-e^{-\psi})}{(1-e^{-\psi})}\frac{1}{\gamma e^{-\psi}} - 1\right] \to c \times \pi \qquad \text{(Eqn 233)}$$

At the recombination, $v_{RE} = 3.015c$ and is trending asymptotically to πc, cf. $v_{\Lambda M} = 3.146c$ and evidently tracking higher at scales beyond z~0.1. A similar effect was found in [III] for visible and SR velocities:

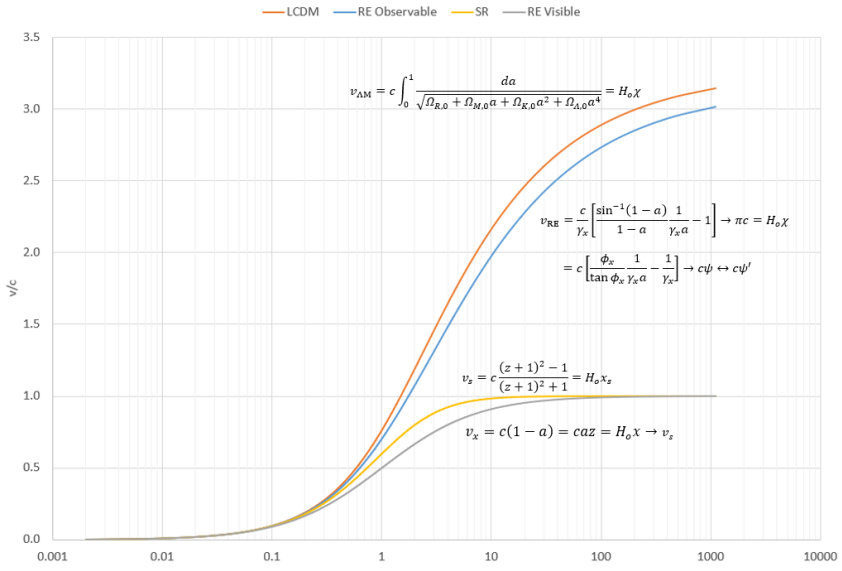

Figure 30: *Comparison of* ΛCDM *and polar* (RE) *observable and visible distance/velocity metrics. Redshift z constructs a coordinate ψ and recession velocities at visible and observable scales. polar visible and* SR *are theories of empirical data, while polar observable and* ΛCDM *are inferred. Visible velocities are limited by lightspeed, while observables are dominated by energies or equivalent accelerations that converge to independent maxima with contraction-dilation greater than* 3c.

The analytic scheme in Figure 30 compares a numerical integration (Table 1) of the ΛCDM model (as parameterised above) to a direct calculation of the π-integral conformal factor:

$$v_{\Lambda M} = H_o\chi = c\int_{a_r}^1 \frac{da}{\sqrt{\Omega_{R,0}+\Omega_{M,0}a+\Omega_{K,0}a^2+\Omega_{\Lambda,0}a^4}} = \text{Table 1 (no direct solution)} \qquad 240$$

cf

$$v_{\text{RE}} = c\left[\sin^{-1}\left(1-e^{-\psi}\right) - \sqrt{2e^{-\psi}-e^{-2\psi}} + \frac{\sin^{-1}\left(1-e^{-\psi}\right)}{1-e^{-\psi}}\right] \qquad \text{(Eqn 234)}$$

The ψ coordinate is calculated from the scale factor, in turn calculated from redshift:

$e^{-\psi} = a = (z+1)^{-1}$ scale factor from cosmological redshift data 241

$\psi = -\ln(a) = 7.004 \ @ \ a = 0.0009083$ coordinate by scale factor at recombination 242

The polar Conformal Scale Factor is then calculated by Eqn 233 on that coordinate (Table 1):

Table 1: Computational comparison of ΛCDM *and polar observable cosmologies. See Figure 31. The observable coordinate ψ is computed on the scale factor. Observable distance and velocity metrics are computed on the coordinate then compared to a separate* ΛCDM *integration.*

Thermal scale factor a	Redshift $z = a^{-1} - 1$ **(plot axis)**	Time integation step size T_f	Distance-velocity integration step size D_f	**ΛCDM Conformal Scale Factor (plot)**	Thermal scale factor $a^{3/2}$	Time scale factor $a\sqrt{2a-a^2} = a/\gamma_x$	Proper Co-moving coordinate ψ	Recession γ_x	**Polar Conformal Scale Factor (plot)**
0.0009083	1099.92	4.67E-05	5.14E-02	**3.1456492**	2.738E-05	3.871E-05	7.0038991	23.47	**3.0151181**
0.0019074	523.27	1.19E-04	8.93E-02	3.0942795	8.331E-05	1.178E-04	6.2620011	16.20	2.9591929
0.0029065	343.05	2.11E-04	1.21E-01	3.0563189	1.567E-04	2.214E-04	5.8407999	13.13	2.9172379
0.0039056	255.04	3.18E-04	1.48E-01	3.0248369	2.441E-04	3.448E-04	5.5453417	11.33	2.8822904
0.0049047	202.89	4.39E-04	1.73E-01	2.9973541	3.435E-04	4.852E-04	5.3175613	10.11	2.8517597
…									
0.1637602	5.11	7.88E-02	1.35E+00	1.8011431	6.627E-02	8.980E-02	2.41017	1.82	1.6263626
0.1647593	5.07	7.95E-02	1.35E+00	1.796768	6.688E-02	9.060E-02	2.40132	1.82	1.6222610
0.1657584	5.03	8.02E-02	1.36E+00	1.7924066	6.749E-02	9.140E-02	2.39252	1.81	1.6181745
…									
0.9960036	0.00	9.47E-01	3.14E+00	0.0050107	9.940E-01	9.960E-01	0.0040043	1.00	0.0040070
0.9970027	0.00	9.48E-01	3.1426473	0.0040055	9.955E-01	9.970E-01	0.0030017	1.00	0.0030032
0.9980018	0.00	9.49E-01	3.1436494	0.0030019	0.9970042	9.980E-01	0.0020001	1.00	0.0020008
0.9990009	0.00	9.50E-01	3.1446500	0.0019997	0.9985017	9.990E-01	0.0009995	1.00	0.0009997
1.0000000	0.00	9.51E-01	3.1456491	**0.000999***	1	1.000E+00	0.00	1.00	0.00

* ΛCDM numerical closure error ~ 0.001 on this integration scheme

The polar visible and SR graphs in Figure 30 use distance and velocity laws on the light cone:

$v_s = c\frac{(z+1)^2-1}{(z+1)^2+1} = H_o x$ SR *distance/velocity based on redshift* (Eqn 201)

$v_x = c\left(1-e^{-\psi}\right) = H_o x$ RE *distance/velocity based on co-moving coordinate* ([I] Eqn 44)

Note that the SR redshift is a Lorentz-Doppler effect, while the proper polar visible is Doppler only. This alone is sufficient to account for the larger velocities and distances predicted by standard model:

$a_{\text{SR}} = \frac{f_o}{f_s} = \sqrt{\frac{1-v_s/c}{1+v_s/c}} = \gamma(1-v_s/c)$ SR *Doppler-relativistic scale factor* 243

$a_{\text{RE}} = \frac{\lambda_s}{\lambda_o} = \frac{s}{s_o} = e^{-\psi} = (1-v_x/c)$ RE *Doppler scale factor* 244

This is suitable for a comparison of polar and standard model theories and data.

[II] Observable Space: Volume, Mass and Energy Integration

Expressions for energy and energy density are evaluated as a sum to total critical density, leading to general relativistic solutions of quantifiable forms of mass-energy. The expansion-kinetic and gravitational-potential energies of the polar metric are evaluated on the assumption that a balance of kinetic and potential is a physically convergent outcome of wave dynamics in expansion. An exact Friedmann critical density derives from this analysis, re-confirming the coordinate velocity form of the Hubble factor. This formulation of critical density includes an inverse square law that overcomes cube-law volume dilution by an ongoing evolution and accumulation of relativistic mass-equivalents of kinetic and potential energies.

These components are evaluated by a quadratic sum to critical density, the solution giving theoretical K and P densities that are within 5% of the ΛCDM *proportions of dark energy and dark matter. The discrepancy is resolved by including galactic kinetic energies, i.e. all forms of kinetic energy, as components of dark energy. This step produces accurate density ratios*

with directly soluble formulae for baryonic matter densities at cosmological and intergalactic scales, the second and third of a series of proof-of-concept waypoints pursued in this research.

Distributions of mass and energy are developed on an expanding system with trial flat and spherical symmetries and variable density, resolved as an equidistant projection in [III]. Beginning with an analysis of cosmological volume under comparative physical assumptions, symmetries are selected from alternatives by conformance to kinetic and potential energy balance. Alternatives capable of this balance become candidates. The lead candidate geometry reproduces a conformal co-moving radius as the hemi-circumference of an observable manifold, corresponding to πS where S is the Hubble radius. This is accurate to within 1.6% of the standard model co-moving radius, leading to reliable expressions for total universal volume, density, mass and kinetic–potential energies due to expansion and gravitation.

In Figure 19 an element or shell of volume dV_r of the 4-space is indicated by a spherical surface at a radius r about an observer in any 3D direction. This radius is a scaled past distance conforming to an equidistant present co-moving distance $r_o = S_o\psi$, that is an arc length on an angular coordinate ψ. This amounts to a re-analysis of the FLRW metric in equidistant polar coordinates. A unrolling 3-sphere in action is equivalent to the extended geometry:

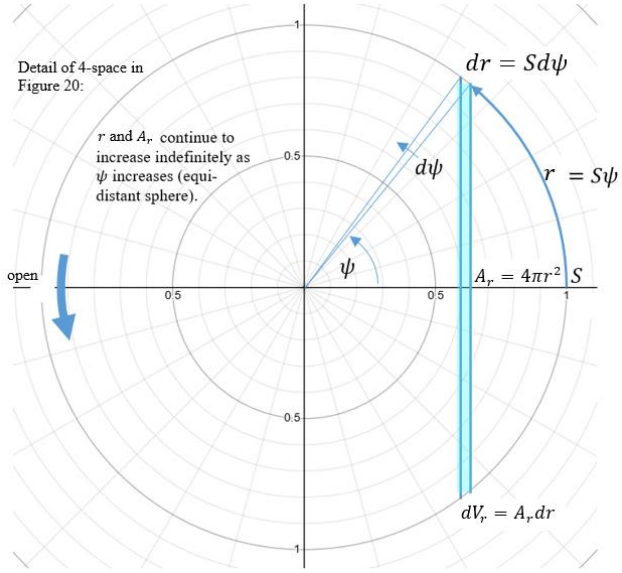

Figure 19: *Equidistant 3-spherical geometry with an open antipode and Euclidean area-volumes at radial distance r.*

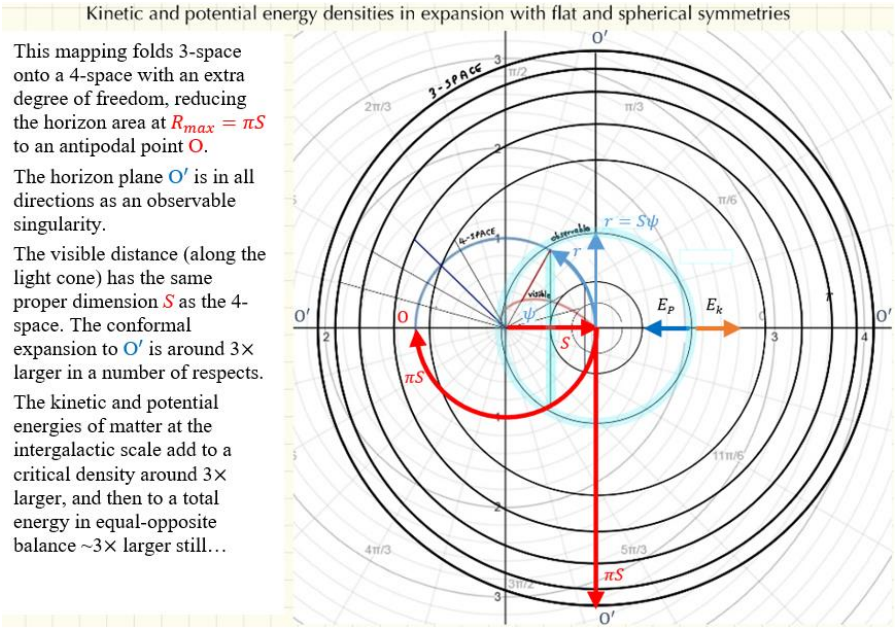

Figure 20: *Unrolled in equidistant projection, observable distances expand to ~3x the corresponding visible distances. The antipode O is the horizon area O′ mapped to a point. Potential and kinetic energies are indicated on this diagram, also around ~3x larger than total critical mass-energy. The positive and negative roles of kinetic and gravitational energy lead to opposite polarities; kinetic and potential are inflationary, increasing with radius by r^{-2} dilution as critical density persists.*

This incorporates the arc theorem with flat distance-area laws on any radius r in a 3D manifold:

$$dV_r = A_r dr = 4\pi r^2 dr = 4\pi(S\psi)^2 S d\psi = 4\pi S^3 \psi^2 d\psi \qquad \textit{Volume element} \qquad 103$$

This implies a 3D polar space with co-moving angular coordinates ψ and a monotonically increasing flat area. This is the logical inverse of an FLRW 3-sphere: an open 3-sphere unrolls or decompactifies to infinite coordinates on a flat volume with a spherical frame. Assuming for now a relative observable spherical limit at $\psi = \pi$ [III, IV]:

$$V_r = 4\pi S_o^3 \int_0^\pi \psi^2 d\psi = 4\pi S_o^3 \left[\frac{\psi^3}{3}\right]_0^\pi = \frac{4}{3}\pi^4 {S_o}^3 = \frac{4}{3}\pi(\pi S_o)^3 \qquad \textit{Observable Volume} \qquad 104$$

The total volume at $\psi = \pi$ is a Euclidean sphere of co-moving radius $r_{max} = R = \pi S_o$ (to 4 sig figs from [I])

$$V_R = \frac{4}{3}\pi(\pi 1.366 \times 10^{26})^3 = \mathbf{3.31 \times 10^{80}}\ \text{m}^3 \qquad \textit{Polar Volume} \qquad 105$$

This is within 4% of the current standard conformal cosmological volume on co-moving coordinates. The volume and its integration conform to a dimensional series for n-spheres $A^n = rC^n/(n+1)$ where C and A are corresponding circumference and area, area and volume, then volume and hypervolume. Assuming conventional ΛCDM gravitational and dark dynamics in the observed acceleration [IV], the Euclidean volume of the observable universe is based on the co-moving radius:

$$\chi = \frac{c}{H_o}\int_0^1 \frac{da}{\sqrt{\Omega_{R,0}+\Omega_{M,0}a+\Omega_{K,0}a^2+\Omega_{\Lambda,0}a^4}} = \frac{2.998\times10^8}{2.175\times10^{-18}}[3.145] = 4.34 \times 10^{26}\ \text{m} \qquad \text{(Eqn 237 [III])} \qquad 106$$

$$V_\Lambda = \frac{4}{3}\pi(4.34 \times 10^{26})^3 = \mathbf{3.43 \times 10^{80}}\ \text{m}^3 \qquad \textit{standard model cosmological volume} \qquad 107$$

For such a simple model, V_R (polar) is very similar to V_Λ (standard model). This parallel of ordinary geometry to general dynamics is intrinsically worth examining.

Volumetric-Dynamic Analysis: Cosmological Mass and Energy

Apparent Kinetic Energy in Observable Space

A generalised kinetic energy of mass expansion relative to the observer can be defined in terms of the kinematics of observable space shells, assuming only that co-moving recession velocities are physically relative [III]. It is not a necessary condition that recession is a relative velocity [3] or that it represents real energy [25]. However on the expectation that inflationary energies have kinetic effects such as acceleration, plausible kinetic energies in the classical sense may be measured as scaled proxies of virtual or dark kinetic effects:

e.g. $dE_k = \frac{1}{2}v_r^2 dM$ *simplest recession kinetic energy element* 108

Where v_r is the observable recession velocity and dM is the element of mass in dV:

For $r_o = S_o\psi$ or $r = S\psi$ with ψ constant (co-moving): 109

$$v_r = \frac{dr}{dt} = \frac{\partial r}{\partial S}\frac{dS}{dt} = \psi c \qquad \textit{observable recession velocity (superluminal for } \psi > 1) \qquad 110$$

This observable recession velocity follows the Hubble law with the same (as in [I]) present value of the constant:

$$v_r = c\psi = c\frac{r}{S} = Hr = c\frac{r_o}{S_o} = H_o r_o \qquad \textit{observable Hubble recession} \qquad 111$$

dM is found by integrating density-volume elements. Without assuming any density except that it is homogeneous and isotropic in large-scale co-moving observable space:

$$dM = \rho dV = \rho A_r dr = \rho 4\pi r^2 S d\psi = \rho 4\pi (S\psi)^2 S d\psi = \rho 4\pi S^3 \psi^2 d\psi \qquad 112$$

We can assemble these terms to integrate the supposed recession kinetic energy:

$$dE_k = \frac{1}{2}v_r^2 dM = \frac{1}{2}(c\psi)^2 \rho 4\pi S^3 \psi^2 d\psi = 2\pi c^2 \rho S^3 \psi^4 d\psi \qquad 113$$

This can be integrated to the horizon at $\psi = \pi$, giving a hypothetical total expansion kinetic energy of observable space:

$$E_k = 2\pi c^2 \rho S^3 \int_0^\pi \psi^4 d\psi = 2\pi c^2 \rho S^3 \left[\frac{\psi^5}{5}\right]_0^\pi = \frac{2}{5}\pi^6 c^2 \rho S^3 \qquad \textbf{\textit{Expansion } } \boldsymbol{E_k} \qquad \mathbf{114}$$

This is the total observable expansion kinetic energy of a hypothetical polar universe of any present density. The model proportionality to ρS^3 may be modified by volume dilution or other effects on ρ.

Apparent Potential Energy in Observable Space

Gravitational potential energy is obtained by a similar integration, leading to an identifiable balance of energies:

$$dE_p = -\frac{GM(r)}{r}dM \qquad \textit{Potential energy element} \qquad 115$$

This is the weak-field gravitational potential energy of a sphere of radius $r = S\psi$ and enclosed mass $M(r)$:

$$M(r) = \int_0^\psi dM = \rho 4\pi S^3 \int_0^\psi \psi^2 \mathrm{d}\psi = \rho\frac{4}{3}\pi S^3 \psi^3 \qquad 116$$

The potential energy can be assembled and integrated:

$$dE_p = -\frac{G\rho\frac{4}{3}\pi S^3\psi^3}{S\psi}\rho 4\pi S^3 \psi^2 d\psi = -G\rho^2\frac{16}{3}\pi^2 S^5 \psi^4 d\psi \qquad 117$$

Total potential energy is then

$$E_p = -G\rho^2\frac{16}{3}\pi^2 S^5 \int_0^\psi \psi^4 d\psi = -G\rho^2\frac{16}{3}\pi^2 S^5 \left[\frac{\psi^5}{5}\right]_0^\pi = -G\rho^2\frac{16}{15}\pi^7 S^5 \qquad \textbf{\textit{Gravitation } } \boldsymbol{E_p} \qquad \mathbf{118}$$

Evolving Critical Density

In a flat universe with optimal escape expansion at critical density (edge of gravitational collapse), potential would be equal and opposite to kinetic energy, even by proxy. Therefore setting the K and P terms equal and opposite:

$$E_p = -G\rho^2\frac{16}{15}\pi^7 S^5 = -E_k = -\frac{2}{5}\pi^6 c^2 \rho S^3 \qquad \textit{Energy Balance} \qquad 119$$

This balance occurs at a theoretical critical density that is identical to standard-model (Friedmann) GR cosmology:

$$G\rho^2\frac{16}{15}\pi^7 S^5 = \frac{2}{5}\pi^6 c^2 \rho S^3 \qquad 120$$

$$G\rho\frac{8}{3}\pi S^2 = c^2 \qquad 121$$

or $$\rho = \frac{3c^2}{8\pi G S^2} = \frac{3H^2}{8\pi G} = \rho_c \qquad \textit{Critical Density} \qquad 122$$

The substitution $c/S = H$ is supported in this model by the analysis in [I], and tends to confirm that [I, II] are based on the same underlying projection [III]. This is the exact form of critical density as it occurs in weak field general relativity. Critical density is more generally obtained from the Friedmann equation for the flat case and solves as:

$$\rho_c = \frac{3H^2}{8\pi G} \qquad \textit{Friedmann Critical Density} \text{ (GR/Newtonian)} \qquad 123$$

Critical Density as Inverse Square

An implication of density converging on critical is that it evolves with the changing squared Hubble parameter, not by volume dilution but by an inverse square law. The missing dimension produces a total mass that must increase in proportion to Hubble radius *if* critical density is sustained:

$$\rho_c = \frac{3H^2}{8\pi G} = \frac{3c^2}{8\pi G S_0^2} \qquad 124$$

This is the critical density of present-valued cosmological time t_o. In past time the critical density varies inversely with S^2:

$$\rho_{c,S} = \frac{3c^2}{8\pi G S^2} = \frac{3c^2}{8\pi G S_0^2 e^{-2\psi}} \qquad 125$$

As a result the mass sum of critical density over universal volume in any cosmological instant increases with radius, that is with forward time. This could only arise in an inflationary process. The system would increase in kinetic energy, but by increasing in relativistic mass equivalent, not by cosmological acceleration.

$$M_r = \rho_{c,S} V_r = \frac{3c^2}{8\pi G S^2}\frac{4}{3}\pi^4 S^3 = \frac{c^2\pi^3}{2G}S = \frac{(c\pi)^3}{2G}t \qquad \textit{evolving mass} \qquad 126$$

This is a convergent limit state, not necessarily operating in or near this state throughout all time or towards zero time: the conserved mass would reduce to a primordial mass of baryonic matter as it persists into the present. Even so, at an estimated 4.7% of critical or $1.4\text{x}10^{53}$ kg baryonic matter, the initial density is without limit:

$$\rho_c = \frac{3c^2}{8\pi G S^2} = \frac{3}{8\pi G t^2} \to \infty \text{ as } t \to 0 \qquad 127$$

The present total observable mass at critical density is proportional to Hubble radius:

$$M_c = \frac{3c^2}{8\pi G S_0^2}\frac{4}{3}\pi^4 S_o^3 = \frac{c^2\pi^3}{2G}S_o = \frac{(c\pi)^3}{2G}t_o \qquad 128$$

This can be evaluated as an energy density, noting that most of the total density in the standard model is dark energy:

$$E_c = c^2\frac{c^2\pi^3}{2G}S_o = \frac{c^4\pi^3}{2G}S_o \qquad 129$$

A universe with mass-energy increasing in an inflationary process is consistent with current empirically supported flat cosmologies [48; 49]. In the most probable model, total observable mass including dark matter plus expanding vacuum energy combine to produce critical density to a very high precision, an asymptotic solution driven towards critical by the quantized collapse of inflationary regions. This explanation follows from several lines of evidence but is not supported by vacuum energy calculations that must be in error by at least 120 orders of magnitude [26].

Assuming critical density, the total energy can be evaluated by adding in the kinetic and potential energies of that density. These turn out to be equal-opposite values that are almost 3× larger than the critical energy density:

$$E_p = -G\rho_c^2\frac{16}{15}\pi^7 S_o^5 = -G\left[\frac{9c^4}{64\pi^2 G^2 S_0^4}\right]\frac{16}{15}\pi^7 S_o^5 = -\frac{3\pi^5}{20}\frac{c^4}{G}S_o = -\frac{3\pi^2}{10}E_c \qquad 130$$

$$E_k = \frac{2}{5}\pi^6 c^2 \rho S_o^3 = \frac{2}{5}\pi^6 c^2\left[\frac{3c^2}{8\pi G S_0^2}\right]S_o^3 = +\frac{3\pi^5}{20}\frac{c^4}{G}S_o = +\frac{3\pi^2}{10}E_c \qquad 131$$

Critical kinetic and potential energies increase in proportion to S_o, but are of opposite sign, and cancel. The total mechanical energy of the expansion remains critical, but develops a dynamic movement from potential (which decreases into negative) to kinetic (increases into positive). This has the dynamic of an inertially falling system converting potential energy to kinetic in a gravitational field, but at constant velocity, by increasing in mass.

Sum to Critical Density: Matter Plus Kinetic and Potential Mass-Equivalents

It is significant that the kinetic and potential mass-equivalents of this critical density are around three times larger than the critical mass that produces them. In a physical evolution this would tend to inflate and converge on critical density, where the energies cancel. Higher mass-equivalents would then reduce to zero with no further escalation.

It can be supposed that this convergence is a natural effect of an evolving wave dynamic, in the process forming dominant kinetic and potential energy densities that are prospectively identified with dark energy and dark matter in the observable universe. This would be an emergent physical mechanism for the unexplained dark dynamics. The analysis is repeated in [IV] for the past visible universe, the lightcone being correlated to the physical future.

The following method evaluates the density of baryonic matter plus its own kinetic and potential mass-equivalent energies due to expansion and gravitation, and then further evaluates the higher energies that develop as the total mass plus mass-equivalent expands. These secondary and tertiary mass-energy distributions couple with other general-relativistic masses, developing further potentials and kinetic energies relative to a co-moving observer. The method measures relative energies by proxy of the recession and gravitation of identifiable mass distributions.

Diluted as a homogeneous-isotropic density at the cosmological scale, i.e. averaged over total space inclusive of large void spaces, the extragalactic density and its evolving mass-equivalent by-products are comparable to cosmological densities that sum in the known dark proportions. Arbitrarily denoted $\rho_\ni$ as a partial cosmological density, the extragalactic density is found to be around five times the density of the baryonic matter that produces it, and has higher products that are still more dense. The resulting mix of matter and its developing energies sum to critical such that the highest kinetic and potential energy densities tend toward equal-opposite and vanish, avoiding an escalation.

The sum of these terms is formulated by writing expansion kinetic and gravitational potential densities as linear and quadratic functions (Eqns 114 and 118) of extragalactic density, the three parts summing to critical:

$$\rho_\ni + \rho_P + \rho_K = \rho_c \qquad \textit{extragalactic and cosmological densities sum to critical density} \qquad 135$$

Since extragalactic density includes matter and the kinetic-potential effects of matter, there will be proportions of kinetic and potential as dark components at the extragalactic scale as details within that mixed term. These can be analysed by comparison to the standard sum of baryonic matter, dark matter and dark energy mass-equivalents:

$$\Omega_B + \Omega_{CDM} + \Omega_\Lambda = 1 \qquad \textit{standard-model sum of baryonic matter, dark matter and dark energy} \qquad 136$$

A solution to Eqn 135 is developed and evaluated below. The kinetic and potential terms (Eqns 114 and 118) are linear and quadratic forms of density, which solve with a number of alternative values that can be examined for physical correspondence. The linear equations contain non-linear coupled and expansion-evolving components. Assuming limit convergence, the solution values are compared to energy densities in the modern universe, i.e. the inferred proportions of dark energy and dark matter, and with baryonic matter at cosmological and intergalactic scales. A tested hypothesis resolves equal-opposite energy densities of critical potential and kinetic, which cancel, on positive mass densities that sum to critical at that point:

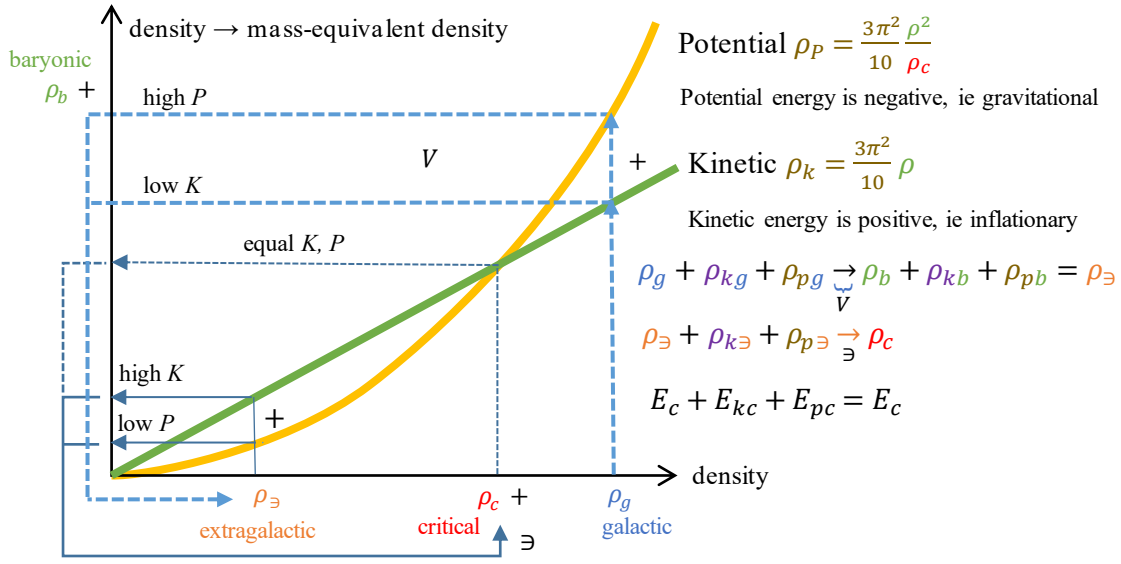

Figure 21: Escalation from galactic baryonic, to cosmological baryonic+mass-equivalent, to critical density. ρ_g is high-density intergalactic matter that develops mass-equivalents of potential and rotation-translation kinetic energies; the total is distributed over volume to the low-density filament-void structure, on large scales reducing to extragalactic equivalent mass density $\rho_\ni$: this mass distribution in turn engages in gravitation and expansion, producing Kinetic and Potential mass-equivalents that sum to critical density ρ_c. Kinetic and potential energies of critical density are then equal-opposite, and cancel. The system would tend to converge to this state, as larger local densities produce higher energies that do not cancel until the cosmological scale accumulates to ρ_c. Intergalactic matter expands and relaxes gravitationally, decreasing in relative potential and increasing in density while expanding; this would arise by accumulating relativistic mass-equivalent.

The model is derived at the cosmological scale; as such there is a risk of scaling errors since the uniformly distributed large-scale cosmological density is far less than the high-density intergalactic and galactic media at smaller scales. This error is tested with similar hypotheses at the intergalactic rather than cosmological scale, providing a good match to the baryonic matter density of the intergalactic medium. Without assuming particles, new or hypothetical (e.g. no need for a messenger graviton) as mass elements, this conserved matter is distinct from higher mass equivalents that behave like matter in their effect on local (galactic) gravitation.

Quadratic Solution of Cosmological Critical Density

Referring back to the kinetic and potential equations for any general density, expansion kinetic energy is directly proportional to mass density ρ while gravitational potential energy is as ρ^2:

$$E_k = \frac{2}{5}\pi^6 c^2 S^3 \rho \qquad \text{(Eqn 114)}$$

$$E_p = -G\frac{16}{15}\pi^7 S^5 \rho^2 \qquad \text{(Eqn 118)}$$

Kinetic mass-equivalent density ($/c^2$) is then proportional to $\rho_\ni$ by the same $\sim 3\times$ constant:

$$\rho_{k\ni} = \frac{M_k}{V_R} = \frac{2}{5}\pi^6 S_o^3 \rho_\ni \frac{c^2}{c^2}\frac{3}{4\pi^4 S_0^3} = \frac{3\pi^2}{10}\rho_\ni \qquad 137$$

Similarly potential energy mass-equivalent is a function of $\rho_\ni^2$:

$$\rho_{p\ni} = -G\frac{16}{15}\pi^7 S_o^5 \rho_\ni^2 \frac{1}{c^2}\frac{3}{4\pi^4 S_0^3} = -\frac{8\pi G S_o^2}{3c^2}\frac{3\pi^2}{10}\rho_\ni^2$$

$$= \oplus \frac{3\pi^2}{10}\frac{\rho_\ni^2}{\rho_c} \qquad 138$$

The introduced $\oplus$ is a marked $\pm$ testable hypothesis that potential mass equivalent may be positive or negative, depending on the polarity of gravitation (potential) and expansion (kinetic) effects. Potential energy density is always taken as negative compared to kinetic, but the corresponding mass-equivalent densities may be positive or negative in gravitational effect, which may be resolved by this hypothesis test.

This leads to

$$\rho_\ni + \frac{3\pi^2}{10}\rho_\ni \oplus \frac{3\pi^2}{10}\frac{\rho_\ni^2}{\rho_c} = \rho_c \qquad \textit{extragalactic mass-equivalent equation} \qquad 139$$

This is a quadratic equation with up to four solutions:

$$\rho_\ni = \frac{-\left(1+\frac{3\pi^2}{10}\right) \pm \sqrt{\left(1+\frac{3\pi^2}{10}\right)^2 - 4\left(\oplus\frac{3\pi^2}{10\rho_c}\right)(-\rho_c)}}{\oplus\frac{6\pi^2}{10\rho_c}} \qquad 140$$

$$= \left[-\left(1+\frac{3\pi^2}{10}\right) \pm \sqrt{1 + \frac{(3\oplus 6)\pi^2}{5} + \left(\frac{3\pi^2}{10}\right)^2}\right]\left[\oplus\frac{5}{3\pi^2}\right]\rho_c$$

$$= \ni\, \rho_c \qquad \textit{solution of mass-equivalent equation} \qquad 141$$

The solution, representing the proportion of critical density due to total intergalactic baryonic matter plus kinetic and potential mass-equivalents, at the convergent limit is a fixed proportion of ρ_c that is itself independent of ρ_c.

Evaluating first the positive hypothetical $\oplus$ potential: all masses are positive:

$$\rho_\ni = \left[-\left(1+\frac{3\pi^2}{10}\right) \pm \sqrt{1 + \frac{9\pi^2}{5} + \left(\frac{3\pi^2}{10}\right)^2}\right]\left[\frac{5}{3\pi^2}\right]\rho_c = \{\mathbf{-1.5549}, \mathbf{0.2172}\}\rho_c \qquad 142$$

Then hypothetical $\ominus$ negative potential-mass, i.e potential mass-equivalent of the same sign as potential energy:

$$\rho_\ni = \left[-\left(1+\frac{3\pi^2}{10}\right) \pm \sqrt{1 - \frac{3\pi^2}{5} + \left(\frac{3\pi^2}{10}\right)^2}\right]\left[\frac{-5}{3\pi^2}\right]\rho_c = \{\mathbf{1.0000}, \mathbf{0.3377} = \mathbf{10/3\pi^2}\}\rho_c \qquad 143$$

The bolded terms are candidates for the value of the unknown extragalactic density $\Omega_\ni = \ni$. These results can be examined for consistency and physical interpretation. The results are necessarily set out in detail as all candidates even in rejection can inform the physical interpretation:

$$\rho_\ni = \ni\, \rho_c \text{ by rational selection of } \ni = \begin{Bmatrix} \mathbf{-1.555} & \mathbf{0.217} \\ \mathbf{+1.000} & \mathbf{0.338} \end{Bmatrix} \qquad 144$$

The $\{\mathbf{-1.555}\}$ solution is a purely mathematical result; it does not correspond to a meaningful density fraction.

The unity solution $\{+\mathbf{1.000}\}$ of the $\ominus$ hypothesis corresponds to the previous critical density analysis: positive and negative kinetic-potential masses cancel, since potential is negative, leaving only critical density in the sum.

The remaining candidate solutions $\{\mathbf{0.338}, \mathbf{0.217}\}$, +ve alternatives of the conventional $\pm$ part of the quadratic, are $-$ and $+$ alternatives respectively of the potential mass hypothesis. These are plausible fractions of critical, of the order of 20 to 30%. The known positive gravitation of baryonic + dark matter is 31% of critical, $\mathbf{\Omega_M = 0.31}$.

The $\ni$ solution is not expected to be negative. The $\oplus$ hypothesis concerns the sign of the potential density that would develop on this effective matter density, i.e. primarily expected to be gravitationally positive. Candidate kinetic and potential densities, labelled $\boldsymbol{K}$ and $\boldsymbol{\Pi}$, can be calculated on either of these values:

$$\rho_{k\ni} = \frac{3\pi^2}{10}\rho_{\ni} = \frac{3\pi^2}{10}\ni\,\rho_c = \frac{3\pi^2}{10}\{\,\mathbf{0.338}\quad\mathbf{0.217}\,\}\,\rho_c = \{+\mathbf{1.000}\quad+\mathbf{0.643}\}.\rho_c = \boldsymbol{K}\rho_c \qquad 145$$

$$\rho_{p\ni} = \oplus\frac{3\pi^2}{10}\frac{\rho_{\ni}^2}{\rho_c} = \oplus\frac{3\pi^2}{10}\frac{\ni^2\rho_c^2}{\rho_c} = \oplus\frac{3\pi^2}{10}\{\,\mathbf{0.338^2}\quad\mathbf{0.217^2}\,\}\,\rho_c = \{-\mathbf{0.338}\quad+\mathbf{0.140}\}.\rho_c = \boldsymbol{\Pi}\rho_c \qquad 146$$

where the bolded terms are hypothetical potential and kinetic proportions of critical density. The $-\mathbf{0.338}$ value is the negative potential-mass density, the minus sign introducing by that definition from $\oplus$. This does not resolve the hypothesis since positive and negative values sum to critical density in either case:

$$\mathbf{0.338} + \mathbf{1} - \mathbf{0.338} = \mathbf{1} \quad ; \quad \mathbf{0.217} + \mathbf{0.643} + \mathbf{0.140} = \mathbf{1} \qquad 147$$

All of the energy in the $\ominus$ solution is kinetic, equal to critical. The cancelling values of **0.338** and **–0.338** are unlikely real solutions, but suggest that a negative cosmological potential-mass density would be associated or even equipartitioned with normal scalar matter density. Parts of this natural association might arise in either the $\oplus$ or the $\ominus$ hypothesis. The association seems valid as an exact solution but is not strong. There must be an as-yet undetermined mixture of different energies at the extragalactic scale, which includes orbit and other kinetics.

This weak association in its simplest positive interpretation relates positive potential mass-equivalent to positive gravity, with the normal definition of potential energy in the negative. Considering the opposing polarities of kinetic–potential in the astrophysical escape process, and furthermore in the inflationary process [48], a positive cosmological potential with positive energy-mass, that is positive gravitation, would hypothetically associate positive kinetic energy with negative gravitation.

Since the proportion of kinetic energy at the intergalactic level is small compared to potential due to the higher densities of galactic matter, most of the extragalactic density would be matter plus the potential of matter, however a significant fraction at that scale must be kinetic, with an even larger kinetic fraction at the cosmological scale.

The positive kinetic solution $\rho_{k\ni} = \mathbf{0.643}\rho_c$ is within 4.7% of the known density proportion of dark energy, taken to two significant figures at the latest cited date as $\Omega_\Lambda = \mathbf{0.69}$. A 4.7% correction, if it can be found in intergalactic kinetic energy, would associate all forms of kinetic with inflationary effects.

This correction is expected to correspond to ρ_{kb}, the kinetic energy density of baryonic matter at the extragalactic scale, i.e. averaged as a component of $\rho_{\ni}$ mixed with the known luminous + dust cosmological baryonic matter $\rho_B = \mathbf{0.048}\rho_c$ and the potential density of baryonic matter, ρ_{pb}. Assuming these actual and hypothetical proportions sum to $\ni = \mathbf{0.217}$, the potential can be estimated to 2 significant figures:

$$\rho_{\ni} = \mathbf{0.217}\rho_c = \rho_b + \boldsymbol{\rho_{kb}} + \boldsymbol{\rho_{pb}} = (\mathbf{0.048} + \mathbf{0.047} + \mathbf{0.12(2)})\rho_c \qquad 150$$

then $\rho_{k\ni} + \rho_{kb} = (\mathbf{0.643} + \mathbf{0.047})\rho_c = \rho_\Lambda$ 151

and $\rho_{p\ni} + \rho_{pb} = (\mathbf{0.140} + \mathbf{0.122})\rho_c = \rho_{\mathrm{CDM}}$ *mix accounting of energy densities* 152

A proportion **0.047** is re-accounted from potential to kinetic: this corresponds to the cosmological kinetic energy density ρ_{kB} that is directly due to baryonic galactic and intergalactic matter, and possibly equipartitioned to baryonic matter density at the cosmological scale. This leads to theoretical calculations of intergalactic and cosmological matter densities from first principles, as demonstrated in the following empirical waypoints:

In the following [III] the geometry is further developed in visible and relative terms to show Doppler and Lorentz effects arising due to recession, again assumed to be relative. This can be used to predict physical characteristics such as temperature histories, and is tested against the thermal age of the recombination epoch visible in the CMB. The modified scale factor, while remaining speculative, is examined as a conformal maximally extended model.

[IV] Energy Analysis [II] Part 2: Volume, Mass and Energy of Present Visible Spacetime

The lightcone is analysed for correlations to presently visible data in the present epoch. This is based on the past-time curvature of the open proper cosmos, which has scaled expansion laws for different points of reference; this works out as a structural asymmetry of the inverse square law at great distances, the diluting magnitude effects of which are suggestive of accelerated distance.

The energy analysis in [II] *is extended to this visible (as opposed to observable) spacetime, integrating these effects as they would appear to a specific observer in their own present. Information arrives from a continuum of spacetime distances, which are scaled by expansion and recession to produce simplified but not significantly re-valued energy densities that remain similar to* [II]. *The metric is revisited in the light of this visible energy analysis, leading to a consistent discrete-symmetric cancellation of gravitational acceleration at the cosmological scale, with similar dark components as in* [II] *and a sinusoidal graph of the distance-area law resembling standard* FLRW *models.*

Visible Spacetime Volume, Matter and Energy Distributions

The lightcone and metric are essential transformation laws from the observable manifold to the directly visible physics of expansion, at a continuum of distances and times into the past. All data or evidence used to frame and calibrate a cosmological theory must be immediately visible in the present epoch, which can then be projected theoretically into the physics of past and future observable space. The analysis in [II] has already anticipated what those physics might be. It remains to check that the projection works, which is to demand similar physics in the scaled empirical past of astronomical data, and in particular to expect similar energy densities that a co-dense manifold would project onto a homogeneous 3-space.

The method set out below follows the lead candidate of a set of trial alternative geometries for balanced kinetic and potential energies at critical density, by distributing mass-energy within volumes on scaled distance-area laws:

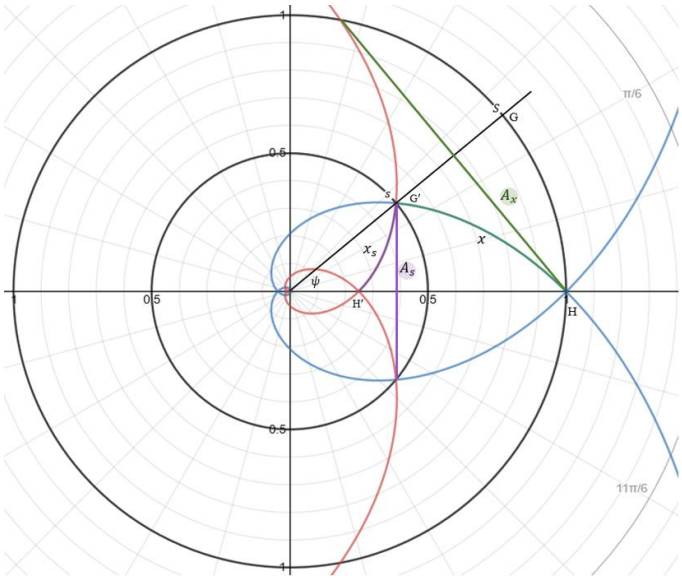

Figure 32: *Physical geometry of visible and observable spacetimes. The distance metric is scaled in area laws and volume elements. The spherical area* A_s *seen by* H *at distance* x *to* G′ *corresponds to the radiated area of light from* H′ *as seen by* G′ *over distance* x_s. *The two definitions agree on the scaled visible area* $A_s = 4\pi x_s^2$ *with a scaled past distance given by* $x_s = S_0 e^{-\psi}(1 - e^{-\psi}) = S(1 - e^{-\psi}) = ax$ *comparing radiation from* G′ *to* H: $A_x = 4\pi x^2$ *along* $r = S_0\psi$.

This suggests a significant modification of the inverse square law, later shown to be consistent with the Friedmann equations. Areas in the distant past visible to an observer are significantly smaller than corresponding areas of radiation or gravitation with area-law dilution around a distant source; this would increase the apparent magnitudes of distant objects, consistent with greater apparent distance due to an equivalent or apparent acceleration.

Volume of Visible Spacetime

The proper scale factor $a = e^{-\psi}$ is essential to the visible area law, in the same sense that the standard-model scale factor is essential to the FLRW metric [III]. Correlation of energies from observable to visible spacetimes depends on a scaled gravitational law that is geometrically similar to a Friedmann equation, producing balanced kinetic and potential energies.

The effect produces a visible kinetic-potential energy balance when critical density varies by an inverse square law into the past. The energy densities are again similar to ΛCDM. The shell area-distance law is again assumed to be Euclidean. The element of distance at x_s is $dx = Sd\psi = cdt$. The visible volume is then:

$$dV_s = A_s dx = 4\pi x_s^2 S d\psi \qquad \textit{visible volume element} \qquad 249$$

$$= 4\pi \left(S_0 e^{-\psi}\left(1 - e^{-\psi}\right)\right)^2 S_0 e^{-\psi} d\psi$$

$$= 4\pi \left(S_0 e^{-\psi}\right)^3 \left(1 - e^{-\psi}\right)^2 d\psi$$

so $$V_s = 4\pi S_0^3 \int_0^\psi e^{-3\psi}\left(1 - e^{-\psi}\right)^2 d\psi$$

$$= 4\pi S_0^3 \int_0^\psi e^{-3\psi} - 2e^{-4\psi} + e^{-5\psi} d\psi$$

$$= 4\pi S_0^3 \left[-\tfrac{1}{3} e^{-3\psi} + \tfrac{1}{2} e^{-4\psi} - \tfrac{1}{5} e^{-5\psi}\right]_0^\psi \qquad 250$$

Assuming $\psi \to \infty$ in visible space:

$$V_s = 4\pi S_0^3 \left[\tfrac{1}{3} - \tfrac{1}{2} + \tfrac{1}{5}\right] = \tfrac{4}{30}\pi S_0^3 \qquad \textit{proper volume of visible space}. \qquad 251$$

This visible volume is $1/10\pi^3$ of the total volume of observable space [II], or $1/10^{\text{th}}$ the volume enclosed by a like 2-sphere.

Mass of Visible Spacetime with Evolving Critical Density

Assuming a constant balance of kinetic and potential energy, critical density must increase into the past by an inverse square law [II]. The total mass again becomes a linear function of S:

$$dM_s = \rho_c dV_s = \frac{3c^2}{8\pi G S_0^2 e^{-2\psi}} 4\pi S_0^3 e^{-3\psi}\left(1 - e^{-\psi}\right)^2 d\psi$$

$$= \frac{3c^2 S_0}{2G} e^{-\psi}\left(1 - e^{-\psi}\right)^2 d\psi \qquad 252$$

Again integrating to $\psi \to \infty$:

$$M_s = \frac{3c^2 S_0}{2G} \int_0^\psi e^{-\psi}\left(1 - e^{-\psi}\right)^2 d\psi$$

$$= \frac{3c^2 S_0}{2G} \left[\tfrac{1}{3}\left(1 - e^{-\psi}\right)^3\right]_0^\psi$$

$$= \frac{c^2 S_0}{2G} = 9.3 \times 10^{52} \text{ kg} \qquad 253$$

This is an inflationary mass including mass-equivalent components, alternatively formulated in time as:

$$M_s = \frac{c^3 t_0}{2G} \qquad 254$$

This result is $1/\pi^3$ of the mass of observable space:

$$M_s = \frac{c^2 S_0}{2G} \qquad \text{cf} \qquad M_R = \frac{\pi^3 c^2 S_0}{2G} \qquad 255$$

Mass in observable and visible space are proportional and scaled to radius S_0.

$$\rho_c V_s = \frac{3c^2}{8\pi G S_0^2} \frac{4}{3} \pi S_0^3 = \frac{c^2 S_0}{2G} \qquad 256$$

The integrated visible mass thus equates to a uniform distribution of present-epoch critical density through an ordinary spherical volume of present Hubble radius: It would be apparent to a present-day observer making or inferring both measurements, that the the total visible mass, including all inferred energies, equals present critical density in a Euclidean volume.

Energy in Visible Spacetime

Kinetic energy relative to the observer along all lines of sight can be integrated through proper visible spacetime:

$$dE_k = \frac{1}{2} v_x^2 dM_s \qquad 257$$

Where v_x is the recession velocity and dM_s is an element of mass in dV_s:

$$v_x = c\left(1 - e^{-\psi}\right) \qquad \text{([I] Eqn 44)}$$

and $$dM_s = \rho_c \, dV_s = \frac{3c^2 S_0}{2G} e^{-\psi} \left(1 - e^{-\psi}\right)^2 d\psi \qquad 258$$

We can assemble these terms to integrate kinetic energy:

$$dE_k = \frac{1}{2} \, c^2 \left(1 - e^{-\psi}\right)^2 \frac{3c^2 S_0}{2G} e^{-\psi} \left(1 - e^{-\psi}\right)^2 d\psi$$

$$= \frac{3c^4 S_0}{4G} e^{-\psi} \left(1 - e^{-\psi}\right)^4 d\psi \qquad 259$$

This produces a simple integrated result:

$$E_k = \frac{3c^4 S_0}{4G} \int_0^{\psi} e^{-\psi} \left(1 - e^{-\psi}\right)^4 d\psi$$

$$= \frac{3c^4 S_0}{4G} \left[-e^{-\psi} + 2e^{-2\psi} - 2e^{-3\psi} + e^{-4\psi} - \frac{1}{5} e^{-5\psi} \right]_0^{\psi}$$

$$= \frac{3c^4 S_0}{4G} \left[\frac{1}{5} \left(1 - e^{-\psi}\right)^5 \right]_0^{\psi} \qquad 260$$

i.e. $$E_k = \frac{3c^4 S_0}{20G} \qquad 261$$

This visible kinetic energy is $1/\pi^5$ of observable kinetic energy [II], numerically similar to the ratio $1/10\pi^3$ of visible and observable volumes, producing similar energy densities as expected.

A similar, balanced potential energy is obtained by the integrating gravitational energies in scaled visible space:

$$dE_p = -\frac{GM_s}{x} dM_s \qquad 262$$

This is the weak-field gravitational potential energy of a spherical shell at visible proper distance $x = S_o\left(1 - e^{-\psi}\right)$ [I]. The inverse distance-potential law uses the unscaled distance x since this is a component of the Hamiltonian in the observer's RF, independent of the area-law metric at distance. The visible mass M_s is integrated as before through scaled shell areas:

$$M_s = \frac{3c^2 S_0}{2G} \int_0^{\psi} e^{-\psi} \left(1 - e^{-\psi}\right)^2 d\psi$$

$$= \frac{3c^2 S_0}{2G} \left[\frac{1}{3} \left(1 - e^{-\psi}\right)^3 \right]_0^{\psi}$$

$$= \frac{c^2 S_0}{2G} \left(1 - e^{-\psi}\right)^3 \qquad 263$$

The total potential energy can then be integrated to any coordinate ψ:

$$dE_p = -\frac{G\frac{c^2 S_0}{2G}\left(1 - e^{-\psi}\right)^3}{S_0\left(1 - e^{-\psi}\right)} \frac{3c^2 S_0}{2G} e^{-\psi} \left(1 - e^{-\psi}\right)^2 d\psi$$

$$= -\frac{3c^4 S_0}{4G} e^{-\psi} \left(1 - e^{-\psi}\right)^4 d\psi$$

$$= -dE_k \qquad 264$$

This integrates as above to give the exact total potential required to balance kinetic energy within proper visible spacetime. The scaled area law has succeeded in defining a potential energy that is equal and opposite to kinetic energy at variable critical density throughout visible space:

$$E_k = -E_p = \frac{3c^4 S_0}{20G} \qquad 265$$

Both potential and kinetic energy are reduced by the same proportion π^5 from their observable counterparts at critical density, a scaling effect numerically similar to the $10\pi^3$ ratio of volumes. The near-unity ratio of these factors leads to simplified exact solutions of Eqn 139 [II] (leads to Eqn 284), re-derived for presently visible data.

This result, the exact formal identity of potential and kinetic energy at critical density, repeats the energy balance found in observable space [II]. This balance is found to occur in visible spacetime *only* on this scaled area law.

Visible Energy Density as Dynamic Pressure in Balance Throughout Visible Spacetime

Again assuming critical density, differential energy and volume elements of visible space form a natural ratio with the form of a dynamic pressure:

$$dE_k = -dE_p = \frac{3c^4 S_0}{4G} e^{-\psi}\left(1 - e^{-\psi}\right)^4 d\psi \qquad \textit{KE = PE with time-varying } \rho_c \qquad 266$$

$$dV_s = 4\pi S_0^3 e^{-3\psi}\left(1 - e^{-\psi}\right)^2 d\psi \qquad \textit{scaled volume} \qquad 267$$

The energy density is the increment of energy per element of volume:

$$\frac{dE}{dV_s} = \frac{3c^4}{16\pi G S_0^2 e^{-2\psi}}\left(1 - e^{-\psi}\right)^2 = \rho_E \qquad \textit{varying energy density} \qquad 268$$

or $$\rho_E = c^2 \frac{\rho_c}{2}\left(1 - e^{-\psi}\right)^2 \qquad 269$$

Noting again the recession velocity ratio $v_x/c = \left(1 - e^{-\psi}\right)$, this amounts to a dynamic pressure:

$$\rho_E = c^2 \frac{\rho_c}{2}\left(\frac{v_x}{c}\right)^2 = \frac{\rho_c v_x^2}{2} \qquad 270$$

This fluid-mechanics result is the density of either kinetic or potential energy. Assuming the negative sign on potential energy, these energy densities sum to zero. The unbalanced virial kinetic components at a lower scale would produce a negative or suction energy in this form of dynamic pressure by recession from the observer.

Critical density generates kinetic and potential energies in equal proportions at any distance, so that a balance of energy is maintained throughout space. To demonstrate this in principle, the differential forms of kinetic and potential are:

$$dE_k = \frac{1}{2} v_x^2 dM_s \qquad 271$$

$$dE_p = -\frac{G M_s}{x} dM_s \qquad 272$$

The relative kinetic/potential rate is found by a simple ratio, cancelling the infinitesimal *dM*:

$$\frac{dE_k}{dE_p} = \frac{v_x^2 x}{-2GM(x)} = \frac{c^2\left(1-e^{-\psi}\right)^2 S_0\left(1-e^{-\psi}\right)}{-2GM(x)} \qquad 273$$

Without assuming a balance, we can evaluate *M*(*x*):

$$\frac{dE_k}{dE_p} M(x) = -\frac{c^2 S_0}{2G}\left(1 - e^{-\psi}\right)^3 \qquad 274$$

This is the same form of M_s found above by integrating inverse-square variable critical density through visible spacetime. This confirms an extended, uniform balance of E_p and E_k:

$$\frac{dE_k}{dE_p} = -1 \qquad 275$$

Potential and kinetic energies are thus in critical balance throughout visible polar spacetime. On this basis it is not necessary to assume anything about a global or universal energy, or that the derived energies at a distance are meaningful in any sense to the local observer, except to say that the energies are locally in balance as measured by other co-moving observers at such distances. If they were added continuously, they would sum to zero.

This tends to mitigate the possible objection that this model may seem to extend a flat space to a global model without formal justification or connection in a GR sense and more particularly that it *depends* on that assumed extension; as shown here, it does not: polar expansion works locally as a plausible solution of GR, with GR-emergent properties, and does not fail globally in either the visible or observable frames.

Extragalactic Density of Proper Visible Spacetime

Given the result that kinetic and potential energy are in constant ratio throughout visible spacetime it is possible to evaluate the distribution of energy mass-equivalent densities as a function of the total mass-equivalent density. This is an essential replication of the extragalactic hypothesis formulated in observable space [II]: the same result must be found in visible spacetime for comparison in any sense to empirical (i.e. presently visible) data.

As before, visible kinetic and potential energies depend on density and density squared:

$$E_k = -E_p = \frac{3c^4 S_0}{20G} \qquad \text{(Eqns 261, 265)}$$

cf $$E_{k,R} = \frac{2}{5}\pi^6 c^2 \rho S_0^3 \qquad E_{p,R} = -G\rho^2 \frac{16}{15}\pi^7 S_0^5 \qquad \text{([II] Eqns 114, 118)}$$

Similar functions of present critical density can be found to extend the ρ and ρ^2 laws to visible space:

$$E_k = \frac{3c^4 S_0}{20G} = k\rho_c \qquad 276$$

$$\rightarrow \quad k = \frac{3c^4 S_0}{20G}\frac{1}{\rho_c} = \frac{3c^4 S_0}{20G}\frac{8\pi G S_0^2}{3c^2} = \frac{2}{5}\pi c^2 S_0^3 \qquad 277$$

This gives the same solution for E_k as in observable space (Eqn 114), again proportional to density and reduced by π^5 from observable to visible. Similarly with potential energy:

$$E_p = -\frac{3c^4 S_o}{20G} = p\rho_c^2 \qquad 278$$

$$\rightarrow \quad p = \frac{3c^4 S_0}{20G}\frac{1}{\rho_c^2} = \frac{3c^4 S_0}{20G}\frac{64\pi^2 G^2 S_0^4}{9c^4} = \frac{16}{15}\pi^2 G S_0^5 \qquad 279$$

This gives the same solution for E_p as in observable space (Eqn 118), again proportional to density-squared and reduced by π^5 from observable to visible.

Still using subscript s to denote terms in visible space, and allowing for the π^5 and $10\pi^3$ projection factors on mass-energy and volume, we have:

$$E_s = \frac{E_R}{\pi^5} \qquad V_s = \frac{V_R}{10\pi^3}$$

$$M_s = \frac{E_s}{c^2} = \frac{M_R}{\pi^5} \qquad \rho_s = \frac{M_s}{V_s} = \frac{M_R}{\pi^5}\frac{10\pi^3}{V_R} = \frac{10}{\pi^2}\rho_R \qquad 280$$

This adjusts the apparent density by a value near 1, since $10 \sim \pi^2$. The same result applies to mass equivalents of potential or kinetic, by the same derivation. This close correlation between observable and visible density provides a simplified calculation of the visible-space density of mass-equivalent, $\rho_\ni$.

The result in observable space was found, with a $\oplus$ hypothesis over positive or negative potential mass-equivalent [II]:

$$\rho_\ni + \rho_k + \rho_p = \rho_c \qquad \text{([II] Eqn 135)}$$

or $$\rho_\ni + \frac{3\pi^2}{10}\rho_\ni \oplus \frac{3\pi^2}{10}\frac{\rho_\ni^2}{\rho_c} = \rho_c \qquad \text{([II] Eqn 139)}$$

In visible space the sum becomes, again on average with uniformly distributed values:

$$\rho_\ni + \rho_{ks} + \rho_{ps} = \rho_c \qquad 281$$

where $\rho_\ni$ and ρ_c are as defined for present observable space, and

$$\rho_{ks} = \frac{10}{\pi^2}\rho_k \quad \text{and} \quad \rho_{ps} = \frac{10}{\pi^2}\rho_p \qquad 282$$

That is $$\rho_\ni + \frac{10}{\pi^2}\left(\frac{3\pi^2}{10}\rho_\ni\right) \oplus \frac{10}{\pi^2}\left(\frac{3\pi^2}{10}\frac{\rho_\ni^2}{\rho_c}\right) = \rho_c \qquad 283$$

or $$\rho_\ni + 3\rho_\ni \oplus 3\frac{\rho_\ni^2}{\rho_c} = \rho_c \qquad 284$$

These simplified density components can also be found by kinetic and potential densities (Eqns 114 and 118 reduced by c^2, π^5 and visible volume):

$$\rho_{ks} = \frac{M_k}{\pi^5 V_s} = \frac{2\pi^6 c^2 S_o^3}{c^2 5\pi^5}\rho_\ni \frac{30}{4\pi S_o^3} = 3\rho_\ni \qquad 285$$

$$\rho_{ps} = \frac{M_p}{\pi^5 V_s} = \oplus\frac{16\pi^7 G S_0^5}{c^2 15\pi^5}\rho_\ni^2 \frac{30}{4\pi S_0^3} = \frac{8\pi G S_0^2}{c^2}\rho_\ni^2 = 3\frac{\rho_\ni^2}{\rho_c} \qquad 286$$

Eqn 139 [II] thus simplifies to

$$\rho_\ni + 3\rho_\ni \oplus 3\frac{\rho_\ni^2}{\rho_c} = 4\rho_\ni \oplus 3\frac{\rho_\ni^2}{\rho_c} = \rho_c \qquad 287$$

This gives a radically simplified but only slightly re-evaluated solution:

$$\rho_\ni = \frac{-4 \pm \sqrt{16 \oplus 12}}{\oplus 6}\rho_c \qquad 288$$

$\oplus$ Positive case: $\rho_\ni = \frac{-4+\sqrt{28}}{6}\rho_c = (\mathbf{-1.548}, \mathbf{0.215})\rho_c$ [compare $(\mathbf{-1.555}, \mathbf{0.217})\rho_c$ in [II]]

$\ominus$ Negative case: $\rho_\ni = \frac{-4-\sqrt{4}}{-6}\rho_c = (\mathbf{1}, \mathbf{1/3})\rho_c$ [compare $(\mathbf{1}, \mathbf{10/3\pi^2})\rho_c$]

This result is an expression of averages, since the bulk density is calculated by total mass per total volume rather than evaluated as variables in ψ, x or s. However the earlier result that kinetic and potential energies remain in balance throughout spacetime ensures that the distribution of energy densities is a constant, conforming in averaged and distributed solutions to:

$$\rho_\ni = \ni\ \rho_c = \frac{-2+\sqrt{7}}{3}\rho_c = \mathbf{0.215}\rho_c \qquad 289$$

This strangely simplified exact (under convergent assumptions) solution is the most direct of several plausible arrangements of this equation (for instance also multiplying $\rho_\ni 10/\pi^2$). To complete this analysis, some important conditions in the proper visible spacetime must now be apparent:

Relationship to FLRW Metric and Friedmann Equation

The proportions of visible spacetime volume, mass and energy are found to be scaled and correlated to observable space. Similar integration constants, $10\pi^3$ and π^5 of volume and energy, derive from the logarithmic geometry of spacetime with

evolving critical density. This produces symmetrical energy densities with a simplified correlation to the mass-equivalent densities of observable space.

This spacetime is geometrically and physically flat in a number of respects. The first is the equality of present critical density to visible mass distributed on a Euclidean volume. This is physically flat and would appear flat to an observer assuming present density and Euclidean geometry at the maximum visible distance:

$$\rho_c V_s = \frac{3c^2}{8\pi G S_0^2}\frac{4}{3}\pi S_0^3 = \frac{c^2 S_0}{2G} = \frac{3c^2 S_0}{2G}\int_0^{\psi} e^{-\psi}\left(1-e^{-\psi}\right)^2 d\psi \qquad 290$$

This Euclidean–polar correspondence would be evident in the data, depending on theoretical interpretations.

Secondly, total energies reduce to zero at critical density [II, IV], which is a physically flat universe in the energetic sense. The solution can evolve asymptotically until no further energies can accumulate, since at critical density they necessarily cancel.

Thirdly, and most significantly, a zero-G dynamic can be derived as a zero-valued Friedmann equation. The acceleration at the edge of a spherical region of arbitrary scaled physical radius r_p around an observer can be constructed by Newtonian gravitation:

$$\vec{g} = \frac{GM}{r_p^2} = \ddot{r}_p \qquad 291$$

In the standard Newtonian-Friedmann derivation, the spherical reference frame around the observer is a scaled spacetime $r_p = ar_i$ in which all mass external to the arbitrary radius cancels as per Newtonian or Poisson-potential gravity. As a result there is conventionally a non-zero acceleration at any finite distance. This external mass cancellation is a general asymmetry of flat space and FLRW models.

An inversion of this general asymmetry arises in polar expansion: the mass outside a spherical shell does not cancel, but the acceleration does. The scaling notation $x_s = ax = S_0 e^{-\psi}\left(1-e^{-\psi}\right)$ is a polar rather than infinite-flat geometry. The Friedmann equation evaluates as zero in this frame.

To see this, consider a galaxy G′ gravitating equally towards remote observers H and H′ at equal and symmetric (isotropic and homogeneous) centres of mass M and M′ (Figure 33). Gravitational effects on G′ arrive from opposite and symmetric distances $x_s = ax$ in both directions, such that gravitational effects are equal and opposite. The resulting balanced accelerations on visible galaxy G′ reduce to zero in any 3-space direction:

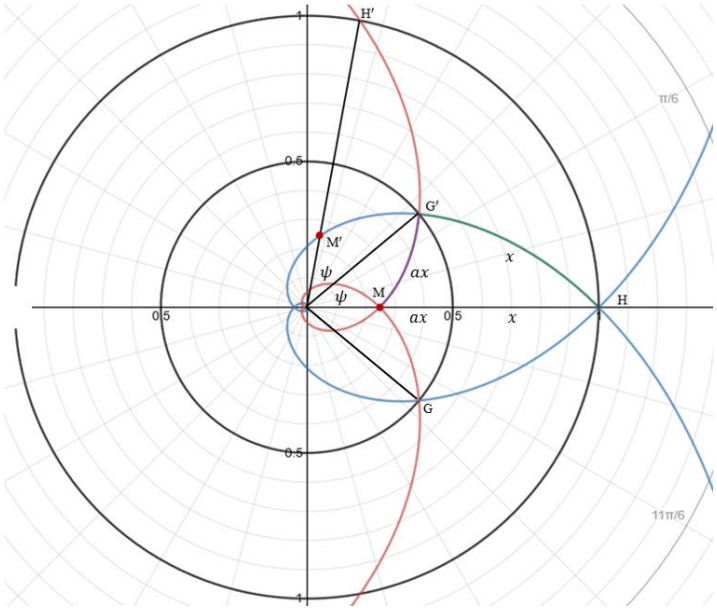

Figure 33: *Symmetric centres of mass at opposite co-moving coordinates produce cancelling gravitational accelerations at any co-moving frame* G − G′. 3D *arc lengths* x *and* ax *correspond to light-distances of radial expansion* ΔS *in two past stages. As a result there is a redshifted scale factor,* $x_s = ax = za^2 ct_0$. *The scaled distance* ax *governs the inverse square law for gravitational effects from the earlier epoch. This is equivalent to a Friedmann equation with a zero solution.*

Initially considered relative to H alone, and assuming only positive gravitational attraction, a galaxy G′ is visible to H at any distance x and accelerates towards the centre of mass M at x' along H's homogeneous past. With no assumption of matter conservation or otherwise into the past, mass M is the centre of gravity of a past spherical matter distribution along a lightcone of scaled radius $x_s = ax$. This is a 3D arc length transmitting a cone of gravitational effects from masses distributed homogeneously around H's worldline reaching all galaxies on the scaled sphere G′ to G. The scaled inverse square then appears in the denominator:

$$\vec{g} = \ddot{x}_s = -\frac{GM}{x_s^2} = -\frac{GM}{a^2x^2} \qquad 292$$

Compare the scaled equation that emerges from infinite polar flat space in the Friedmann equations:

$$a = \frac{r_p}{r_i} \rightarrow \ddot{a} = \frac{\ddot{r}_p}{r_i} \quad \text{since } r_i \text{ is a particular constant depending on choice of initial values.}$$

So $\ddot{a} = \frac{\ddot{r}_p}{r_i} = -\frac{GM}{r_i r_p^2} = -\frac{4\pi}{3}\frac{G\rho_i r_i^3}{r_i r_p^2} = -\frac{4\pi}{3}\frac{G\rho_i r_i^3}{r_i (a r_i)^2} = -\frac{4\pi}{3}\frac{G\rho_i r_i^3}{a^2 r_i^3} = -\frac{4\pi}{3}\frac{G\rho_i}{a^2}$ 293

The acceleration of the scale factor is thus independent of initial radius and depends only on initial density. This guarantees homogeneity since the evolution of the model does not depend on initial radius; the dynamics are independent of any assumed initial volume. This can also be interpreted as an infinite universe since any initial radius, out to any large or infinite initial radius, will behave in the same way.

Then $r_i \ddot{a} = \ddot{r}_p = -\frac{GM}{r_p^2} = -\frac{GM}{a^2 r_i^2}$ 294

With $x_s \equiv r_p$ and $x \equiv r_i$ (Eqn 30 [I] Guth's notation) in the roles of scaled physical distance and present-epoch coordinate distance the gravitational law in polar space scales identically to a Friedmann equation:

$$\ddot{x}_s = -\frac{GM}{a^2 x} = \ddot{a}x \qquad \textit{Polar equivalence to Friedmann I Equation} \qquad 295$$

Now also considering H′ as an equal-mass central RF in the opposite direction beyond G′, we can evaluate this Friedmann equation in both null directions, from G′ towards M and M′ on equal-opposite scaled inverse squares:

$$\ddot{x}_s = -\frac{GM}{a^2 x^2} + \frac{GM'}{a^2 x^2} = 0 \qquad \textbf{\textit{Zero-valued Polar Friedmann I Equation}} \qquad \textbf{296}$$

This cancellation of the Friedmann I equation relies on the directional symmetry of past polar space around the distant reference frame. The object accelerates due to gravity at the inverse square distance visible to that epoch; not the distance at observer H. As a result, relative to H, G′ accelerates symmetrically in all directions.

In the more familiar Newtonian or Poisson potential gradient law, there is an asymmetry between inside and outside a shell, such that gravitational effects cancel from outside the shell, producing a non-zero inward acceleration. This flat spacetime asymmetry does not occur in an equidistant projection, which is linear hence symmetric at distance, such that the shell acceleration vanishes.

The exact symmetry of the acceleration $\vec{g} = 0$ at any distance depends on the scaling of spacetime with distance, so that symmetrical gravitation-cone geometries in the diagram are correct as depicted. For example this would not work in the flat $R = S\psi$ open polar symmetry of observable space as the more distant shell would not be equal, but larger as ψ^2. It would also not work in an orthogonal projection, which is non-linear.

The reducing scale factor controls this overburden, as the visible spacetime area law begins to decrease at radial distances beyond $a = 0.5$: More distant spaces contain smaller volumes, and masses. This resolution derives from the scaled metric, most easily written as an area law, already examined in relation to magnitude effects.

The fourth and final key symmetry derives from the area law:

$$A_s = 4\pi\left(S_0 e^{-\psi}\left(1 - e^{-\psi}\right)\right)^2 \qquad \text{(Eqn 245)}$$

where $x = S_0\left(1 - e^{-\psi}\right)$

and $e^{-\psi} = 1 - \frac{x}{S_0}$

The area law then becomes:

$$A_s = 4\pi\left(x\left(1 - \frac{x}{S_0}\right)\right)^2$$

$$= 4\pi\left(x - \frac{x^2}{S_0}\right)^2 \qquad 297$$

As the co-moving coordinate reduces to visible distance by scale factor, the area law reduces to a squared quadratic with maximum area at $x = S/2$ (Figure 34). A symmetrical flat universe with FLRW-like metric arises within visible space:

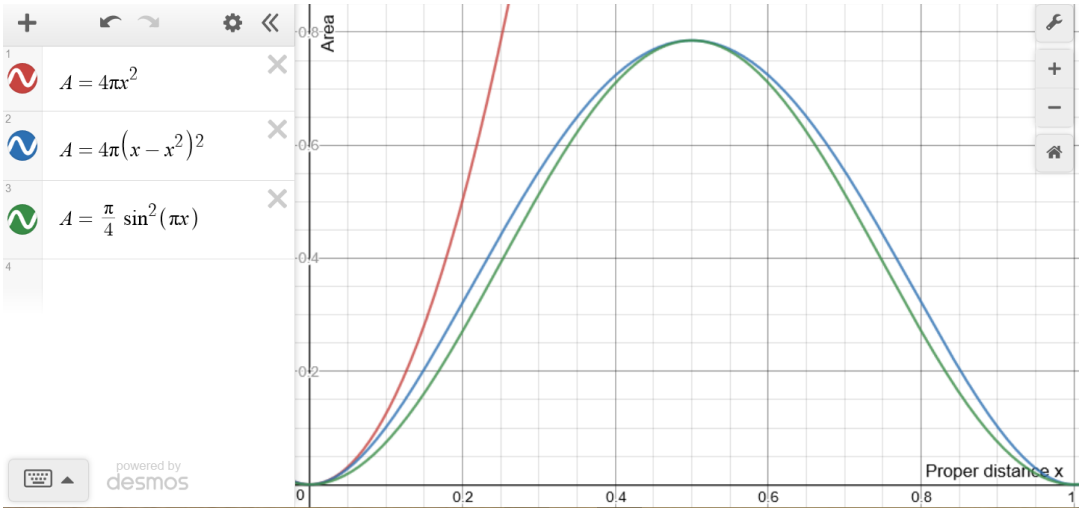

Figure 34: *Cosmological area law on proper distance* x *in scaled visible spacetime* (blue) *compared to inferred visible* (red) *and a simplified* FLRW (green). *The horizontal x axis is normalised to proper* $x_{max} = S_0 = 1$. *The area law is a symmetrical fourth-power polynomial with similar quadratic properties near* $x = 0$ *and* $x = S_0$. *The symmetry derives from the*

complementary of $x + S = S_0$. *The overall symmetry is similar to the* FLRW *metric, but produces flat geometry at distances measured by* CMB *data.*

As with the FLRW metric, the maximum area occurs at half the maximum distance $x = S_o/2$, and reduces to zero in near space and at the horizon. Differentiating visible area by distance:

$$A_s = 4\pi\left(x - \frac{x^2}{S_0}\right)^2$$
$$\frac{dA_S}{dx} = 8\pi\left(x - \frac{x^2}{S_0}\right)\left(1 - \frac{2x}{S_0}\right)$$
$$= 0 \;@\; x = 0\,, \frac{S_0}{2}\,, S_0 \qquad 298$$

It can be seen that maximum area occurs at $x = S_0/2$, with minima at $x = (0, S_0)$.

The value of the maximum area is:

$$A_{max} = 4\pi\left(\frac{S_0}{2} - \frac{S_0^2}{4S_0}\right)^2$$
$$= 4\pi S_0^2\left(\frac{1}{2} - \frac{1}{4}\right)^2$$
$$= \frac{\pi S_0^2}{4} \qquad 299$$

This is the surface area of a Euclidean sphere with radius one quarter the Hubble radius, corresponding to the maximum relativistic visible distance [III] at a circumferential distance to the horizon:

$$x'_{max} = \pi r'_{max} = \frac{\pi S_0}{4} \qquad \text{[III] (Eqn 222)}$$

This would indicate no empirical inconsistency between the maximum relativistic distance and the corresponding maximum Euclidean spherical area. This is a flat geometric result, assuming only those physical descriptions. In fact the maxima occur at different distances and the maximum distance rolls up into an area-point mapping interpreted physically as a singularity.

Differentiating again, it becomes evident that the area curve is symmetrical:

$$\frac{dA_S}{dx} = 8\pi\left(x - \frac{3x^2}{S_0} + \frac{2x^3}{S_0^2}\right)$$
$$\frac{d^2A_S}{dx^2} = 8\pi\left(1 - \frac{6x}{S_0} + \frac{6x^2}{S_0^2}\right)$$
$$= 0 \;@\; x = \frac{S_0}{2}\left(1 \pm \sqrt{\frac{1}{3}}\right) \qquad 300$$

The symmetry derives from the complementarity of S and x: this can be shown by comparing the area function by the complementary mapping $x = S_o - S$:

$$A_s = 4\pi\left(x - \frac{x^2}{S_0}\right)^2 = 4\pi\left((S_0 - S) - \frac{(S_0 - S)^2}{S_0}\right)^2 = 4\pi\left(S - \frac{S^2}{S_0}\right)^2 \qquad \mathbf{301}$$

The surprising result is that the scaled spherical area at a distance around an observer is equal to the corresponding area on the Hubble radius at that distance, i.e. a 2-sphere centred on the complement to distance $S = S_0 - x$ at any visible coordinate. This is a strange enlargement of the object-observer symmetries of the standard inverse square law.

The involution of visible area resembles an FLRW metric governed by scale factor and Hubble radius rather than by a sine function of the distance. This is a natural concluding point for the formulation of a polar metric, reducing to zero at S_o.

The zeroing effect is dependent on this past visible FLRW-like spacetime. The FLRW-like metric cancels the external mass overburden, reducing it to a symmetrical balance of potential and kinetic energies and cancelling gravitational acceleration on the cosmological scale. In both related senses, the universe is flat, but based on a spherical metric.

This conclusion supports the wave-like physics of zero cosmological acceleration in this theory.

Overall Conclusions on Polar Expansion Theory

This zero-acceleration theory cannot be dismissed on the same terms as failed empty-universe or matter-dominant theories, which use the theoretical structure of ΛCDM on empirically eliminated parameter ranges. The parameters of the polar model do not depend on those energies, but use the redshift data to calculate physical coordinates and then use those coordinates to inertially model distances, velocities and densities.

Dark matter is identified as the multiple-generation mass-equivalent of gravitational potential energy, generated by the expansion of conserved baryonic matter in its own energetic gravitational field. The quantum description of this virtual matter has not been addressed, however in a general field theory the inflationary mass field would be only initially localised in the baryonic matter, and thereafter subject to diffusive physics [e.g. 9] of the associated wave-particles. Dark matter would tend to diffuse in a cloud around galaxies and undoubtedly contributes to their evolution. Excesses of the mass-equivalent might be associated with higher degrees of gravitational relaxation, suggesting a further empirical test of dark matter on galactic data sets [II].

Dark energy is similarly identified as an effect, rather than a cause, of the kinetic energies of polar expansion. Assuming an underlying energetic process driving an efficient conversion of potential to kinetic energy, the inflationary energy would be in proportion to its kinetic effects. The quantum description of this effect has been attempted by Ernest [1]. Conservation of energy with cancelling inflationary effects must require a theoretical energy in the range of the empirical data; this solution is found by direct computation, with no errors of magnitude. The method needs no new particles or new physics: it does this by further generalising GR to allow coupling of cosmological densities that generate higher cosmological densities, which avoid a crisis by converging to critical.

These energies, which are defined by constant velocity, are not associated with cosmic acceleration. Gravitational acceleration at the largest scale reduces to zero. This is shown to be consistent with the standard-candle evidence of acceleration, which is explained as a dilation effect due to recession, further generalising GR to allow this as for any relative velocity. The energies measured in ΛCDM are assumed to increase with increasing velocity. The polar model, based on a wave physics paradigm, finds the same kinetic energies increase at constant velocity by increasing in mass and density. Smaller proper velocities compared to ΛCDM are consistent with this.

The milder kinematics of polar expansion are consistent with a constant velocity due to wave motion. The theoretical departure occurs at the same redshift $z \sim 0.1$ as in the departure of ΛCDM from closed or flat universe models. These earlier models are to that extent more consistent with polar expansion than ΛCDM. It must be re-asserted that the standard model cannot be entirely complete or correct in its present form. The CMB dipole cannot be explained by ΛCDM or matter-dominant models, likewise there are significantly different estimates of the Hubble constant due to evident inconsistencies in alternative modes of calculation from standard-model first principles.

This model begins with an implausibly simple premise, that the unknown dark components of cosmology, along with some of the intractable contradictions of general relativity with quantum mechanics, may be soluble by re-framing the physics of expansion to include a wave behaviour along with a gravitational "particle" behaviour. This is not something that can be proven mathematically, but matches a large part of the data and provides consistent explanations [I to IV].

How then does this model map to the metrics of general relativity at the scale of stars and black holes? The uniform symmetries of gravity at the cosmological scale, which allow any number of maximally extended Minkowski models, are not allowable at any real lower scale.

The objection here is that this theory has no integral step in the formulation of the cosmological metric from the special-relativistic and particle-based locally inertial spacetime, and no recognition of the medium-scale inhomogeneity of gravitational timescapes [e.g. 3] up to the filament-void scale. This research has assumed a constant lightspeed in every sense, including that of expansion without embedding into a 4th space dimension. Given a coherent original source, the only possible manifold at equal speed in all dimensions is spherical. The timescape is assumed to be inherent in the manifold as an accumulation of kinetic SR and potential GR curvatures that are continually updated onto the manifold by interference at the particle scale. This is empirically Riemannian since particle and electromagnetic effects are contained within the manifold, so there is no physical or measurable embedding of the manifold within any higher geometry, unless it is by direct detection of graviton particles with properties hypothetically requiring a higher dimension.

The 3-spherical wavefront depicted in Figures 1 and 2 is intended to hold at any scale as a segment of an open sphere in 4-space, as in Figures 17 and 18 [I]. Special relativistic proper times and distances can be constructed in the 4-dimensional wave-space inheriting the 3D parallel volume [I, III]. General Relativistic metrics match the data, however they have not been re-derived for this projection, so they may have no theoretical basis. Nevertheless the non-linearity of Huygens' principle in any even number of space dimensions suggests that non-linear, self-coupling actions on proper times and distances may also result due to gravity without necessarily altering the 3-spherical wavelet structure at local scales, since the Huygens-Fresnel model is non-linear in four (even) space dimensions. That proposition has manifestly *not* been tested in this thesis.

The existence of a range of cosmological solutions in general relativity, of which the flat case is only one solution and neither special nor likely (or even stable without inflationary help) stands against the evidence that the universe is and probably *must be* a flat solution. The flat universe is a convergent empirical result, and not coincidental, that denies the possibility of open and closed universes in any completely correct theory. Classical open and closed universes are now more or less unthinkable on the evidence, yet they arise in the same fundamental theory that supports the FLRW and ΛCDM models.

As shown, the inferred accelerations and energies of the dark modern universe can be explained by a constant, uniform radiation and expansion of electromagnetic and gravitational effects with equal and constant velocity. This reduces to just two differential Eqns 31 and 32, which derive at the very least a good approximation of the empirical universe in observable, proper and visible spacetimes. Explaining this simplifying convergence by a well-constituted quantum field theory, going beyond the elementary calculus derivations of this thesis, is a major next step requiring an extension of this research beyond the author's present ability.

As with the Kaluza-Klein and Milne theories, this model produces a match to empirical relativistic cosmology, but again comes at the expense of gravitational dynamics on the cosmological scale. Not necessarily accepting this, but certainly exploring and deconstructing this model should be regarded as a significant challenge for modern physical cosmology.

[I – IV] References

[1] Ernest, A.D. 2012. *Does Quantum Wavepacket Expansion Influence Cosmic Evolution?* Proc. Australian Institute of Physics Congress, Sydney Dec 2012

[2] Barrow, J. 2011. *The Book of Universes; Exploring the Limits of the Cosmos.* W.W.Norton & Co.

[3] Wiltshire, D.L. 2007. *Cosmic clocks, cosmic variance and cosmic averages*. gr-qc/0702082; New J. Phys. 9 (2007) 377 (Focus on Dark Energy)

[4] Huygens, C. 1678 *Traite de la Lumiere.* (Monograph, 1690 Leiden: Pieter van der Aa)

[5] Hadamard, J. 1923. *Lectures on Cauchy's problem in linear partial differential equations*. Yale University Press, New Haven.

[6] Epstein, L.C. 1983. *Relativity Visualised*. Insight Press, ISBN 0-935218-03-3

[7] Fresnel, A. 1819. *Memoire sur la diffraction de la Lumiere.* Mémoires de l'Académie des sciences, tome V, pp.339-475

[8] Kirchhoff, G. 1883. *Zur theorie der Lichtstrahlen.* Ann. d. Physik. **254** (4): 663–695

[9] Gottwald, G.A. and Melbourne, I. 2013. *A Huygens principle for diffusion and anomalous diffusion in spatially extended systems.* Proc. Natl. Acad. Sci USA 110(21):8411-6. doi: 10.1073/pnas.1217926110. Epub 2013 May 7

[10] Enders, P. 2009. *Huygens Principle as Universal Model of Propagation.* Lat. Am. J. Phys. Educ. Vol. 3, No. 1, Jan. 2009 **PACS:** 11.10.-z, 41.85.-p, 42.15.-i, 42.15.Dp **ISSN 1870-9095**

[11] de Broglie, L-V. 1925. *Recherches sur la Th'eorie des Quanta.* Ann. de Phys. 10ᵉ série t. III

[12] Schwarzschild, K. 2016. *On the gravitational field of a mass point according to Einstein's theory.* Sitzungsber.Preuss.Akad.Wiss.Berlin (Math.Phys.) 189-196 arXiv:physics/9905030v1 [physics.hist-ph]

[13] Guth, A. 2014. *The Early Universe* MIT Open Courseware, ITunes U.

[14] Susskind, L. 2013. *Cosmology.* The Theoretical Minimum Lectures, Stanford University http://theoreticalminimum.com/courses/cosmology/2013/winter accessed March 2017

[15] Harrison, E.R. 1981 *Cosmology; The Science of the Universe* 2nd Edn. CUP

[16] Finelli, F. Gruppuso, A. Paci, F. Starobinsky AA. 2012. *Searching for hidden mirror symmetries in CMB fluctuations from WMAP 7 year maps* JHEP 07 (2012) 049 http://arxiv.org/abs/1111.5362v2

[17] Terrell, J. 1959 *Invisibility of the Lorentz Contraction*. Phys. Rev. **116**, 1041

[18] Weisskopf, V.F. 1960 *The Visual apperarance of rapidly moving obects*. Physics Today

[19] de Sitter, W. 1917. *On the curvature of space,* Proc. Kon. Ned. Acad. Wet. **20**: 229–243

[20] Slipher, V.M. 1913. *The radial velocity of the Andromeda nebula*. Lowell Observatory Bulletin, **2**, 56-57

[21] Slipher, V.M. 1917. *Nebulae*. Proc. Amer. Phil. Soc. **56**. 403-409

[22] Friedmann, A. 1922. Über die Krümmung des Raumes. *Zeitschrift für Physik*, **10**, 377-386

[23] Lemaître, G. 1927. *Un univers homogène de masse constante et de rayon croissant, rendant compte de la vitesse radiale des nébuleuses extra-galactiques*. Annales de la Société scientifique de Bruxelles, Série A, 47, 49-59.

[24] Hubble, E. 1929. *A Relation between Distance and Radial Velocity among Extra-Galactic Nebulae.* Proc. National Academy of Sciences of the United States of America, Volume 15, Issue 3, pp. 168-173

[25] Sandage, A. 1962 *The Change of Redshift and Apparent Luminosity of Galaxies due to the Deceleration of Selected Expanding Universes* Astrophysical Journal **136** 319-333 *Bibcode:1962ApJ...136..319S. doi:10.1086/147385*

[26] Carroll, S.M. 2004. *Spacetime and Geometry; An Introduction to General Relativity.* Addison Wesley ISBN 0-8053-8732-3.

[27] Milne, E.A. (1940). *Cosmological Theories*, Ap.J. 91:129-158

[28] Cane, F. 2015. *Intergalactic Space*. Astronomy Today. http://www.universetoday.com/30280/intergalactic-space/ https://space.fandom.com/wiki/Intergalactic_space

[29] Ryden, B. 2006. *Introduction to Cosmology*. Ohio State University Department of Astronomy

[30] Condon, J. 2016. *Cosmic Microwave Background Radiation* National Radio Astronomy Observatory Lecture notes for ASTR534 Essential Radio Astronomy http://www.cv.nrao.edu/course/astr534/CMB.html

[31] Hyperphysics; Astrophysics; Redshift; http://hyperphysics.phy-astr.gsu.edu/hbase/astro/redshf.html#c1 Accessed June 2017

[32] Ringemacher H.I and Mead L.R. 2015. *Model-independent Plotting of the Cosmological Scale Factor as a Function of Lookback Time*. arXiv:1407.6300v2 [astro-ph.CO] AJ 148, 94 (2014)

[33] Daly, R.A. and Djorgovski, S.G. 2004. *Direct Determination of the Kinematics of the Universe and Properties of the Dark Energy as Functions of the Redshift.* The Astrophysical Journal 612 (2), 652-659

[34] S. Perlmutter, G. Aldering, G. Goldhaber and others. 1999. *Measurements of Ω and Λ from 42 High-redshift supernovae*. The Astrophysical Journal, 517 : 565, 586

[35] Riess, A.G. et al. 1998. *Observational Evidence from Supernovae for an Accelerating Universe and a Cosmological Constant* The Astronomical Journal **116**:1009-1038

[36] Hawking, S. 1988. *A Brief History of Time.* Bantam Books

[37] Davis, T.M and Lineweaver, C.H. 2001. *Superluminal Recession Velocities.* arXiv:astro-ph/0011070v2

[38] Christoffel, E.B. 1869, *Uber die Transformation der homogen Differentialausdrücke zweiten Grades.* Journal für die reine und angewandte Mathematik, **70**: 46–70

[39] Davis, T.M. and Lineweaver, C.H. 2003. *Expanding Confusion: common misconceptions of cosmological horizons and the superluminal expansion of the Universe*. Pub. Aust. Soc. Aust.

[40] Einstein, A. and de Sitter, W. 1932. *On the relation between the expansion and the mean density of the universe.* Proceedings of the National Academy of Sciences. ***18** (3): 213–214.*

[41] Einstein, A. 1916. *The Foundation of the General Theory of Relativity*. IN: The Collected Papers of Albert Einstein, Vol. 6. Kox, A.J. Klein, M.J. and Schulmann, R. (Eds) 1997, Princeton University Press

[42] Roukema, BF, Ostrowski, JJ, Buchert, T, 2013. *Virialisation-induced curvature as a physical explanation for dark energy*. arXiv:1303.4444v3 [astro-ph.CO]

[43] T Buchert, M Carfora, G F R Ellis, E W Kolb, M A H, MacCallum, J J Ostrowski, S Räsänen7, B F Roukema, L Andersson, A A Coley, and D L Wiltshire. 2015. *Is there proof that backreaction of inhomogeneities is irrelevant in cosmology?* arXiv:1505.07800v2 [gr-qc]

[44] Baker, B.B and Copson, E.T 1950. *The Mathematical Theory of Huygens' Principle.* 2nd Edn. OUP, London

[45] Brown, K. 2017. *Huygens Principle*. http://www.mathpages.com/home/kmath242/kmath242.htm accessed September 2018

[46] Rovelli, C. 2010. *Quantum Gravity*. Cambridge University Press. Online ISBN 9780511755804

[47] Carroll, S.M. *From Eternity to Here.* Penguin, USA.

[48] Krauss, L.M. 2012 *A Universe from Nothing* Simon & Schuster ISBN 978-1-47111-269-0

[49] Planck Collaboration, 2018. *Planck 2015 Results VI. Cosmological Parameters* arXiv:1807.06209v1

[50] Davies, P. 1984. Superforce; *The Search for a Grand Unified Theory of Nature* Unwin Hyman

[51] Kaluza, Theodor 1921. *"Zum Unitätsproblem in der Physik"*. Sitzungsber. Preuss. Akad. Wiss. Berlin. (Math. Phys.): 966–972.

[52] Verlinde, E.P. 2016. Emergent Gravity and the Dark Universe. arXiv:1611.02269v2

[53] Thiry, M.Y. 1948. *Compt. Rend. Acad. Sci.* Paris **226**: 216–218.

[54] Healey, R. 2007. *"Gauging What's Real: The Conceptual Foundations of Contemporary Gauge Theories."*

[55] Straumann, N. 1998. *Early History of Gauge Theories and Kaluza-Klein Theories, with a Glance at Recent Developments* http://www.researchgate.net/publication/2041194

[56] Weatherall, J.O. 2014 (in press). *"Fiber Bundles, Yang-Mills-Theory, and General Relativity"*. http://philsci-archive.pitt.edu/11146/1/Fiber_bundles_YM_and_GR.pdf UCLA Irvine

[57] Randall, L. and Sundrum, R. 1999. *An alternative to compactification.* Physical Review Letters. 83 (23): 4690–4693. arXiv:hep-th/9906064 Oxford University Press, New York.

[58] Schwarz, DJ, Copi CJ, Huterer, D. and Starkman, GD. 2016 *CMB Anomalies after Planck.* Classical and Quantum Gravity

[59] Tomozawa, Y. 2018. *CMB Dipole, Peculiar Velocity and Hubble Flow*. arXiv:0705.1317v1

[60] Scott, D. 2001. *CMB: Frequently Asked Questions*. www.astro.ubc.ca/people/scott/cmb

[61] Itoh, Y., Yahata, K. and Takada, M. 2010. *A dipole anisotropy of galaxy distribution: Does the CMB rest-frame exist in the local universe?* Phys.Rev.D82:043530,2010 arXiv:0912.1460 [astro-ph.CO]

[62] Copi, C. and Starkman, G.D. 2022. *Gravitational Glint: detectable gravitational wave tails from stars and compact objects.* arXiv:2201.03684v1 [gr-qc]

[63] Carroll, Sean M. 2022. *From Eternity to Here. Z The Quest for the Ultimate Theory of Time.* Dutton. ISBN 978-0525951339

[64] Gerghetta, T. 2006. "Warped Models and Holography". in *Particle Physics beyond the Standard Model*. Kazakov, D. Lavignac, S. and Dalibard, J. (Eds). Les Houches **86**: 263-265, 267-311